ORIGINAL RESEARCH
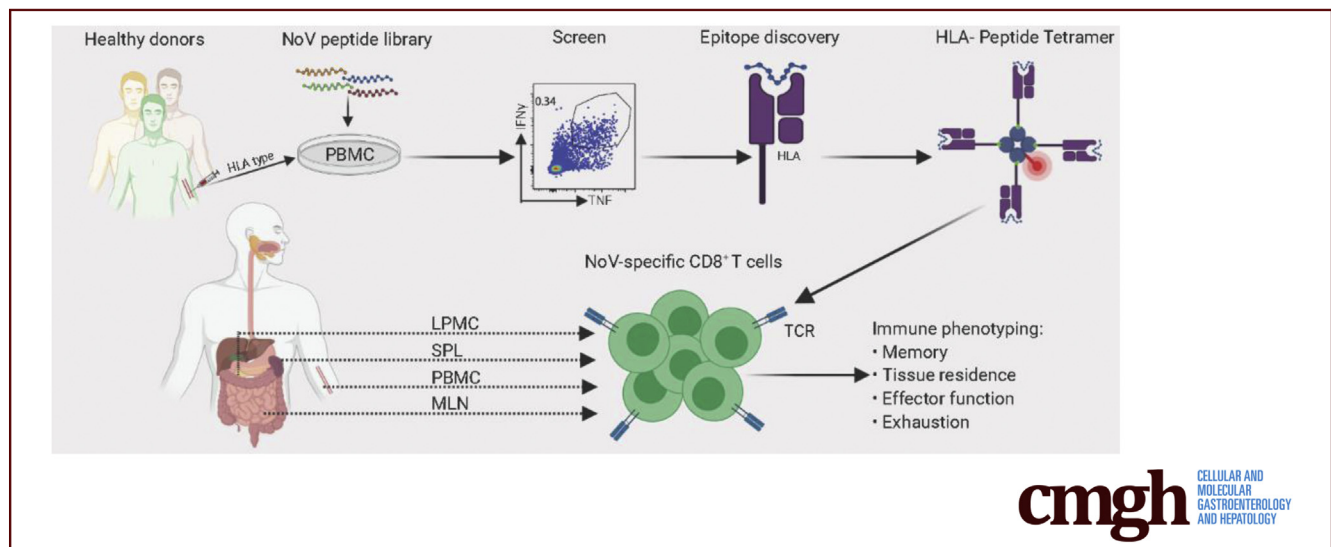
Norovirus-Specific CD8$^+$ T Cell Responses in Human Blood and Tissues

Ajinkya Pattekar,[1] Lena S. Mayer,[1,2] Chi Wai Lau,[1] Chengyang Liu,[3] Olesya Palko,[1,4] Meenakshi Bewtra,[1,5] HPAP Consortium,[6] Lisa C. Lindesmith,[7] Paul D. Brewer-Jensen,[7] Ralph S. Baric,[7] Michael R. Betts,[8] Ali Naji,[3] E. John Wherry,[9,10,11] and Vesselin T. Tomov[1,10]

[1]Department of Medicine, Division of Gastroenterology, Perelman School of Medicine, University of Pennsylvania, Philadelphia, Pennsylvania; [2]Department of Medicine II: Gastroenterology, Hepatology, Endocrinology, and Infectious Disease, University Medical Center Freiburg, Freiburg, Germany; [3]Department of Surgery, Perelman School of Medicine, University of Pennsylvania, Philadelphia, Pennsylvania; [4]Department of Orthopedic Surgery, Montefiore Medical Center, Bronx, New York; [5]Center for Clinical Epidemiology and Biostatistics, Perelman School of Medicine, University of Pennsylvania, Philadelphia, Pennsylvania; [6]The Human Pancreas Analysis Program (RRID:SCR_016202); [7]Department of Epidemiology, University of North Carolina, Chapel Hill, North Carolina; [8]Department of Microbiology, Perelman School of Medicine, University of Pennsylvania, Philadelphia, Pennsylvania; [9]Department of Systems Pharmacology and Translational Therapeutics, Perelman School of Medicine, University of Pennsylvania, Philadelphia, Pennsylvania; [10]Institute for Immunology, University of Pennsylvania Perelman School of Medicine, Philadelphia, Pennsylvania; and [11]Parker Institute for Cancer Immunotherapy, University of Pennsylvania Perelman School of Medicine, Philadelphia, Pennsylvania

SUMMARY

Conserved HLA class I epitopes were defined by screening a norovirus peptide library. HLA-peptide tetramers tracked norovirus-specific CD8$^+$ T cells with diverse differentiation states across lymphoid and intestinal tissues. These reagents can enhance future vaccine studies and cell-based treatment approaches.

BACKGROUND & AIMS: Noroviruses (NoVs) are the leading cause of acute gastroenteritis worldwide and are associated with significant morbidity and mortality. Moreover, an asymptomatic carrier state can persist following acute infection, promoting NoV spread and evolution. Thus, defining immune correlates of NoV protection and persistence is needed to guide the development of future vaccines and limit viral spread.

Whereas antibody responses following NoV infection or vaccination have been studied extensively, cellular immunity has received less attention. Data from the mouse NoV model suggest that T cells are critical for preventing persistence and achieving viral clearance, but little is known about NoV-specific T-cell immunity in humans, particularly at mucosal sites.

METHODS: We screened peripheral blood mononuclear cells from 3 volunteers with an overlapping NoV peptide library. We then used HLA-peptide tetramers to track virus-specific CD8$^+$ T cells in peripheral, lymphoid, and intestinal tissues. Tetramer$^+$ cells were further characterized using markers for cellular trafficking, exhaustion, cytotoxicity, and proliferation.

RESULTS: We defined 7 HLA-restricted immunodominant class I epitopes that were highly conserved across pandemic strains from genogroup II.4. NoV-specific CD8$^+$ T cells with central, effector, or tissue-resident memory phenotypes were present at

all sites and were especially abundant in the intestinal lamina propria. The properties and differentiation states of tetramer^{+} cells varied across donors and epitopes.

CONCLUSIONS: Our findings are an important step toward defining the breadth, distribution, and properties of human NoV T-cell immunity. Moreover, the molecular tools we have developed can be used to evaluate future vaccines and engineer novel cellular therapeutics. *(Cell Mol Gastroenterol Hepatol 2021;11: 1267–1289; https://doi.org/10.1016/j.jcmgh.2020.12.012)*

Noroviruses (NoVs) are highly infectious and resilient pathogens and the leading cause of acute gastroenteritis worldwide.[1,2] Annually, an estimated 267 million NoV infections lead to more than 200,000 deaths, with the highest morbidity and mortality among the elderly, immunocompromised, and young children in developing countries.[3] In the United States alone, NoV gastroenteritis leads to nearly 1 million health visits and significant economic losses annually.[4] Currently, there are no approved pharmacologic therapies against NoV, and despite several promising clinical trials, an effective vaccine is not available.[5,6]

NoVs are non-enveloped, single-strand positive sense RNA viruses belonging to the *Caliciviridae* family. The viral genome is ∼7.6 kilobases long, and in the case of human strains, it is organized into 3 overlapping open reading frames (ORFs). ORF1 encodes a polyprotein that self-cleaves into 6 mature nonstructural proteins including an NTPase (NS3), protease (NS6), and RNA-dependent RNA polymerase (NS7).[7] ORF2 encodes the major structural protein, VP1, which self-assembles into 90 dimers to form the viral capsid.[8] VP1 contains a conserved shell (S) domain and a protruding (P) domain. The P domain in turn consists of a stalk (P1) region and an exposed hypervariable (P2) region that mediates attachment to host cells and is the primary target of neutralizing antibodies.[1] ORF3 encodes the minor structural protein, VP2, which enables release of the viral genome from the capsid upon cellular entry.[9]

The NoV genus is phylogenetically complex with up to 10 genogroups and 49 genotypes that are based on amino acid diversity of VP1.[10] Multiple human strains occupy genogroups I, II, and IV and more than 30 genotypes,[10] leading to frequent exposures and seropositivity rates among adults of greater than 90%.[11] Despite this high genetic diversity, all 6 NoV pandemics since 1996 were caused by genetically related members of genogroup II, genotype 4 (GII.4).[12] These variants differed primarily in P2, the hypervariable region of VP1 that mediates binding to ABH histo-blood group antigens (HBGAs) on host cells. HBGAs are important NoV infectivity determinants that enable viral attachment to host cells in a strain- and host-specific manner.[13] Thus, antibodies that block P2-HBGA interactions correlate with protection, but most are variant-specific, reflecting immune-driven viral evolution.[12,14] Broadly reactive antibodies that target conserved epitope in the P1 and S domains have also been

described, particularly across GI genotypes,[15] but they do not neutralize GII variants.[1,16] Conversely, genetic mutations in HBGA synthesis pathways can be broadly protective by preventing NoV binding to epithelial cells. For example, polymorphisms in the *FUT2* gene lead to a defective $\alpha(1,2)$ fructosyltransferase in up to 20% of white individuals.[17] Such individuals, termed *non-secretors*, cannot produce the carbohydrate H type-1 on epithelial cells and are naturally resistant to GI.1 and GII.4 NoVs, although they remain susceptible to NoVs from several other genogroups.[18]

Although the binding patterns and cross-reactivity of NoV-specific antibodies have been characterized extensively, the overall protective capacity and durability of humoral immunity have been harder to define.[1] Early volunteer studies using high NoV challenge titers suggested that preexisting antibodies correlated with protection in some but not all individuals, and the longevity of such protection was on the order of weeks to months.[19–21] More recent data using smaller challenge doses to reflect natural exposure, as well as mathematical modeling, have shown that NoV immunity is more durable and could last for years.[22,23] Observations from vaccine trials have further shown that antibody titers after immunization correlate with protection upon homologous challenge.[24,25] In one of these trials, the overall infection rates in the vaccine and placebo groups were 61% and 82%, respectively, suggesting that immune mechanisms other than antibodies may be important for protection against NoVs.[24]

Compared with humoral immunity, cellular immunity has received little attention despite evidence from the mouse NoV (MNV) model of the importance of T cells in viral clearance and protection.[26] Volunteers infected with a GII.2 virus exhibited a predominantly Th1 immune response that was cross-reactive against GI.1 and GII.1 virus-like particles (VLPs) in ex vivo assays.[27] In similar experiments, peripheral blood mononuclear cells (PBMCs) from volunteers infected with a GI.1 strain reacted to VLPs from GI.1, GI.2, GI.3, and GI.4 variants.[28] These studies were notable for significant variation in the T-cell response between volunteers and the near absence of CD8 T-cell responses detected using VLP stimulation. Recently, T cells from a cohort of non-secretors infected with a GII.2 strain were shown to be cross-reactive against GII.4 VLPs, even though these subjects had no preexisting GII.4 immunity.[29]

Most current article

These findings suggest that T cells may target conserved epitopes and could offer cross-protection against a broad range of NoVs.

Specific T-cell epitopes from NoV were initially identified in mice immunized with VLP-expressing viral vectors, followed by ex vivo stimulation with overlapping peptide libraries.[30] Two epitopes, mapping to the P1 and S capsid domains, were discovered and showed high degree of conservation across genogroups and genotypes. Moreover, responses against these epitopes were elicited by a diverse range of VLPs, implying broad cross-reactivity of epitope-specific T cells.[30] Because these epitopes were discovered in mice, their significance to human immunity is less clear. Subsequently, a single HLA-restricted CD8^{+} T-cell epitope was identified by using human PBMCs stimulated with a GII.4 capsid peptide library.[31,32] Recently, Hanajiri et al[33] conducted a comprehensive epitope screen using peptides derived from the GII.4 Sydney 2012 pandemic strain and PBMCs from multiple healthy donors. NoV-specific CD4^{+} and CD8^{+} T-cell responses were elicited by peptide pools from each viral protein and varied among donors. Two NoV proteins, NS6 and VP1, were chosen for detailed mapping and led to the identification of 31 HLA-restricted epitopes. Again, epitope-specific T cells showed cross-reactivity against variant sequences from other NoV strains. Notably, all but 3 of these epitopes were HLA class II restricted, possibly reflecting a paucity of CD8^{+} T-cell epitopes in NS6 and VP1.[33]

Beyond defining immunodominant epitopes for therapeutic purposes, understanding the phenotype, functionality, and localization of virus-specific T cells could shed light on important aspects of NoV-host interactions. For example, although most human NoV infections are brief and self-limited, chronic infections have been repeatedly documented in immunocompetent individuals and likely contribute to viral evolution and spread.[12,34–38] Discovering the cellular reservoir and immune mechanisms that enable such NoV persistence will have important therapeutic and epidemiologic implications. We have used the MNV system to address these questions and found that during chronic infection, virus-specific tissue-resident memory (T$_{RM}$) CD8^{+} T cells in the intestinal lamina propria (LP) followed a unique differentiation program that allowed them to retain effector properties, while apparently ignoring ongoing viral replication.[2] It is likely that this mechanism of immune evasion is related to sequestration of MNV in intestinal tuft cells that serve as an immune-privileged niche for long-term viral persistence.[2,39] A similar mechanism is likely to be at play in humans, although the cellular target for persistent human NoV infection remains unknown,[40] and the T-cell component of the human immune response is largely undefined.

Here we use a NoV peptide library and HLA-typed human PBMCs from 3 healthy donors, including a non-secretor, to identify 7 immunodominant CD8 T-cell epitopes. We show that these epitopes are highly conserved across GII.4 strains and use peptide-HLA tetramer reagents (tetramers) to track and phenotype NoV-specific memory T cells in peripheral blood, lymphoid tissues, and the intestinal LP. Our findings show that circulating and T$_{RM}$ CD8^{+} T cells can be detected in healthy adults and express distinct patterns of tissue residence markers. Moreover, the tissue distribution and phenotype of NoV-specific T cells vary between donors and epitopes, suggesting a range of differentiation states after NoV infection. The molecular tools we have developed can be used to assess responses to NoV vaccination or natural infection and define CD8^{+} T-cell correlates of NoV immunity.

Results

Norovirus-Specific T-Cell Responses Can Be Detected in Blood From Healthy Donors

Peripheral blood samples were collected from 3 healthy adult donors (Table 1) with unknown NoV exposure histories, and the presence of NoV functional antibodies was assessed by measuring binding between VLPs and HBGAs in the presence of serum from each donor.[22] Donor 1 had blocking antibodies against several pandemic GII.4 strains and a GII.17 strain (Figure 1A and D). Donor 2 had a broader antibody repertoire that was active against both GI and GII strains (Figure 1B and D). In contrast to Donors 1 and 2, serum from Donor 3 showed no activity against the strains tested (Figure 1C and D), suggesting that this donor had a limited exposure history and/or was a non-secretor. To further investigate this question, we sequenced the FUT2 susceptibility allele from each donor and confirmed that Donor 3 was homozygous for the G428A nonsense mutation and was therefore a non-secretor and resistant to most GI.1 and GII.4 viruses[18] (data not shown). Therefore, we tested serum from the 3 donors against the GII.2 Chapel Hill strain that can infect non-secretors.[29] Donors 1 and 2 had blocking activity against this GII.2 virus (Figure 1A and B), whereas no activity was detected in the serum from Donor 3 (Figure 1C). These findings further suggested limited NoV exposure of Donor 3, although they did not rule out the possibility that this donor had been exposed to strains that were not represented in our VLP panel, because cross-blockade antibodies, particularly among GII strains, are rare.[1] Next we tested donor PBMCs for NoV-specific T-cell responses using overlapping peptide libraries covering each ORF (Figure 2A). Peptides were 15 amino acids long (15-mers) and overlapped neighbors by 10 residues. Our library was based on the 2002 Farmington Hills GII.4 pandemic strain (GenBank: AY502023),[41] which could be blocked from cellular ligand binding by serum from Donors 1 and 2 (Figure 1A and B). We chose the Farmington Hills strain because we reasoned that adults would have likely had 2002 pandemic strain exposure. Moreover, we chose not to use a more recent strain because we wanted to identify conserved GII.4 epitopes that were not subject to evolution and thus constituted promising vaccine targets that could generate broad immunity across emergent GII.4 strains. To amplify preexisting NoV-specific responses, we first incubated donor PBMCs with all 496 peptides from the 3 libraries and expanded responding cells with interleukin (IL) 2 (Figure 2B). A similar stimulation method has been used to detect cytomegalovirus-specific T cells.[42] We then

Table 1. Donor Demographics

Donor	Age (y)	Sex	HLA A	HLA B	HLA C	Cells/tissues	Cause of death
1	33	Male	11:01; 24:02	40:01; 58:01	03:02; 07:02	PBMCs for library screen and phenotyping	N/A
2	33	Male	24:02; 24:02	07:02; 44:06	05:01; 07:02	PBMCs for library screen and phenotyping	N/A
3	45	Male	11:01; 11:01	35:01; 51:01	04:01; 04:01	PBMCs for library screen and phenotyping	N/A
4	18	Male	02:01; 25:01	07:02; 35:01	04:01; 07:02	MLN, SPL	Cardiac arrest
5	37	Male	02; 03	07; 38	07; 12	LPMCs	Head trauma
6	27	Female	03:01; 68:03	18:01; 35:01	05:01; 07:02	LPMCs	Cardiac arrest
7	26	Female	02:06; 11:01	15:02; 40:01	04:03; 08:01	PBMCs to validate findings from initial screen	N/A
8	?	Male	24; 26	38; 61		PBMCs to validate findings from initial screen	N/A
9	40	Male	01:01; 24:02	08:01; 15:01	03:03; 07:01	PBMCs to validate findings from initial screen	N/A
10	48	Male	02:01; 23:01	07:02; 49:01	07:01; 07:02	PBMCs to validate findings from initial screen	N/A
11	25	Male	34:02; 68:02	07:02; 57:03	07:01; 07:02	PBMCs to validate findings from initial screen	N/A
12	27	Female	01:01; 02:01	07:02; 08:01	07:01; 07:02	PBMCs to validate findings from initial screen	N/A
13	24	Female	02:01	07:02; 15:01	03:04; 07:02	PBMCs to validate findings from initial screen	N/A
14	20	Male	02:01	07:02; 18:01	07:02; 12:03	PBMCs to validate findings from initial screen	N/A
15	41	Male	66; 68	41; 35		PBMCs to validate findings from initial screen	N/A
16	53	Female	29:02; 30:01	35:01;53:01	04:01	PBMCs to validate findings from initial screen	N/A
17	41	Male	02:01; 03:01	35:01; 44:03	04:01; 16:01	PBMCs to validate findings from initial screen	N/A
18	29	Male	01:01; 68:03	35:12; 55:01	03:03; 04:01	PBMCs to validate findings from initial screen	N/A
19	19	Male	01:01; 02:01	08:01; 35:03	04:01; 07:01	PBMCs to validate findings from initial screen	N/A

restimulated PBMCs with smaller peptide pools (or individual candidate peptides) in the presence of brefeldin A and measured interferon gamma (IFN-γ) and tumor necrosis factor (TNF) production by flow cytometry (Figure 2B and C).

T-cell responses induced by stimulation with all 496 peptides were readily detectable and varied in magnitude for individual donors (Figure 2C, column 1). These responses were predominantly CD8+, with only Donor 1 showing a robust CD4+ T-cell response. This likely reflected differences in individual exposure histories, our peptide library design that favored discovery of short (HLA class I) epitopes,[43] and the stimulation conditions that enabled CD8+ T-cell outgrowth. Inter-donor differences were also observed within the CD8 T-cell compartment. Donor 1 had responses directed primarily against ORF1 epitopes, whereas Donors 2 and 3 targeted mainly ORF2 (Figure 2C, columns 2 and 3). Furthermore, these data suggested that Donor 3, who was a nonsecretor and had undetectable serologic responses against the tested strains (Figure 1C), must have been exposed to a non-GII.4 NoV, or another pathogen, that shared CD8 T-cell epitopes with the Farmington Hills strain.[44] Overall, responses were weakest against ORF3. Thus, NoV-specific T cells targeting ORF1 and ORF2 epitopes are present in peripheral blood from healthy donors regardless of secretor status.

Defining Immunodominant T-Cell Epitopes

Having shown CD8+ T-cell responses to large peptide pools, we aimed to define the specific epitopes triggering these responses. For this purpose, we divided the 3

peptide libraries into smaller overlapping pools consisting of 20–25 peptides using a "3-D" matrix layout with each peptide represented in 3 different pools[45] (Figure 3A). We then expanded and stimulated donor PBMCs with these pools as shown in Figure 2B and measured TNF and IFN-γ production (Figure 3B). This allowed us to quickly narrow down the response to individual 15-mers (Figure 3B and C). Candidate peptides were further analyzed by using the Immune Epitope Database (IEDB) Analysis Resource (http://tools.immuneepitope.org)[46] and NetMHCpan method (http://www.cbs.dtu.dk/services/NetMHCpan/)[47] to predict optimal shorter binding sequences (typically 9 or 10 amino acids long) within each 15-mer (Figure 3D).

Using the above strategy, we identified seven 15-mers corresponding to 8 predicted immunodominant epitopes restricted to donor HLA types (Figure 4). On the basis of IEDB predictions, shorter peptides (ranging between 9 and 13 amino acids in length) were further explored to define the optimal immunodominant sequences (Figure 4, data not shown). In Donor 1, the CD8+ T-cell response was driven primarily by peptides 137 (RASGLLHERLDEFEL) and 39 (LHGETFPYTAFDNNC) from ORF1 and peptide 6 (VMALEPVVGAAIAAP) from ORF2 (Figure 4A and D). IEDB analysis of peptide 137 identified 2 possible 9-mers restricted to HLA-B*40:01 (HERLDEFEL) and HLA-C*03:02 (LLHERLDEF), with the former sequence yielding the stronger response. Peptides 39 and 6 contained 9-mers (GETFPYTAF and LEPVVGAAI, respectively) with predicted restriction to HLA-B*40:01 (Figure 4A). In Donor 2, peptide 206 (FWVSPSLFITSTHVI) from ORF1 and peptides 14 (VSPRNAPGEILWASP) and 106 (TLAPMGNGTGRRRAL) from ORF2 accounted for most of the CD8+ T-cell response (Figure 4B). Peptide 206
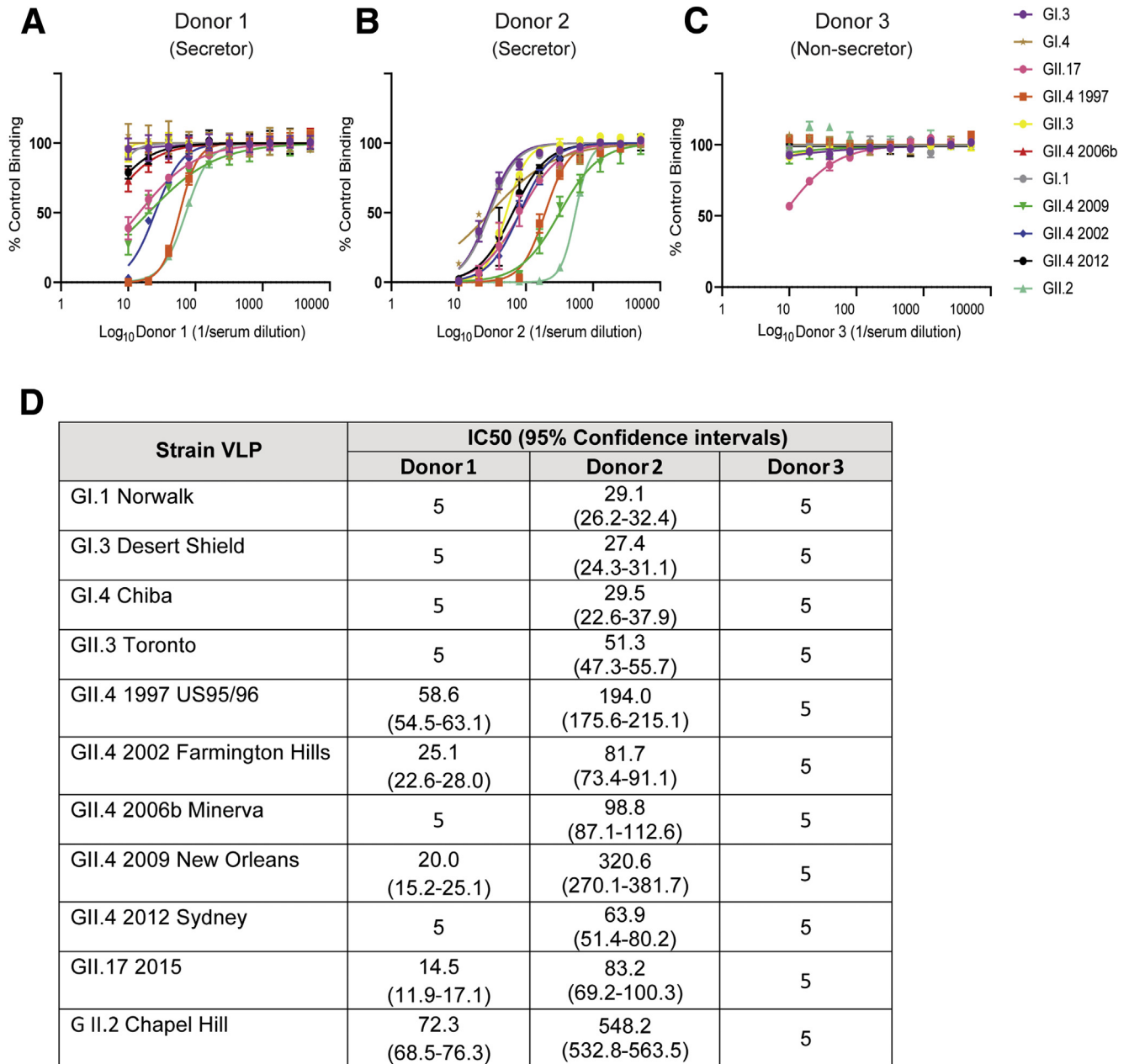
Figure 1. NoV functional antibodies in healthy donors. Serum from 3 healthy adult donors was assessed using a blockade assay that measures the ability of samples to block interaction of VLPs with ligands. A panel of antigenically diverse GI and GII VLPs representing time-ordered pandemic strains was tested. Donors 1 and 2 were secretors (*A* and *B*), whereas Donor 3 was a non-secretor (*C*). Blockade antibody titers and IC50 values (reported in parentheses as reciprocal of the serum dilution 95% confidence interval) are summarized in (*D*). Each sample was assayed in 10-fold serial dilution in minimum of 2 independent experiments.

incorporated a 9-mer (LFITSTHVI) restricted to HLA-A*24:01. Peptides 14 and 106 contained a 10-mer (SPRNAPGEIL) and 13-mer (APMGNGTGRRRAL), respectively, restricted to HLA-B*07:02. Finally, a single immunodominant 9-mer (LPDVRNNFY) derived from ORF2 and restricted to HLA-B*35:01 was identified from Donor 3 (Figure 4*C*).

Consistent with HLA class I binding preferences, most identified epitopes were 9 or 10 amino acids long and contained canonical anchor residues at the second and last positions[43] (Figure 4*D*). Although epitope 106 exceeded the typical length for HLA class I restricted epitopes, epitopes of this length have been described, including ones that bind to HLA-B*07:02.[48] In most cases, the shorter peptides resulted in increased magnitude and/or mean fluorescence intensity of the IFN-γ+ TNF+ signal compared with the parental 15-mers, consistent with improved binding of the optimal HLA-peptide complex to the T-cell

receptor (Figure 4A–C). Epitope 137B was an exception to this rule, yielding a markedly weaker response compared with the parental 15-mer (Figure 4A). This observation suggested that epitope 137A was immunodominant and accounted for most of the signaling response seen with peptide 137 in Donor 1. Thus, our peptide screen identified 8 HLA class I restricted epitopes derived from a GII.4 pandemic NoV strain.
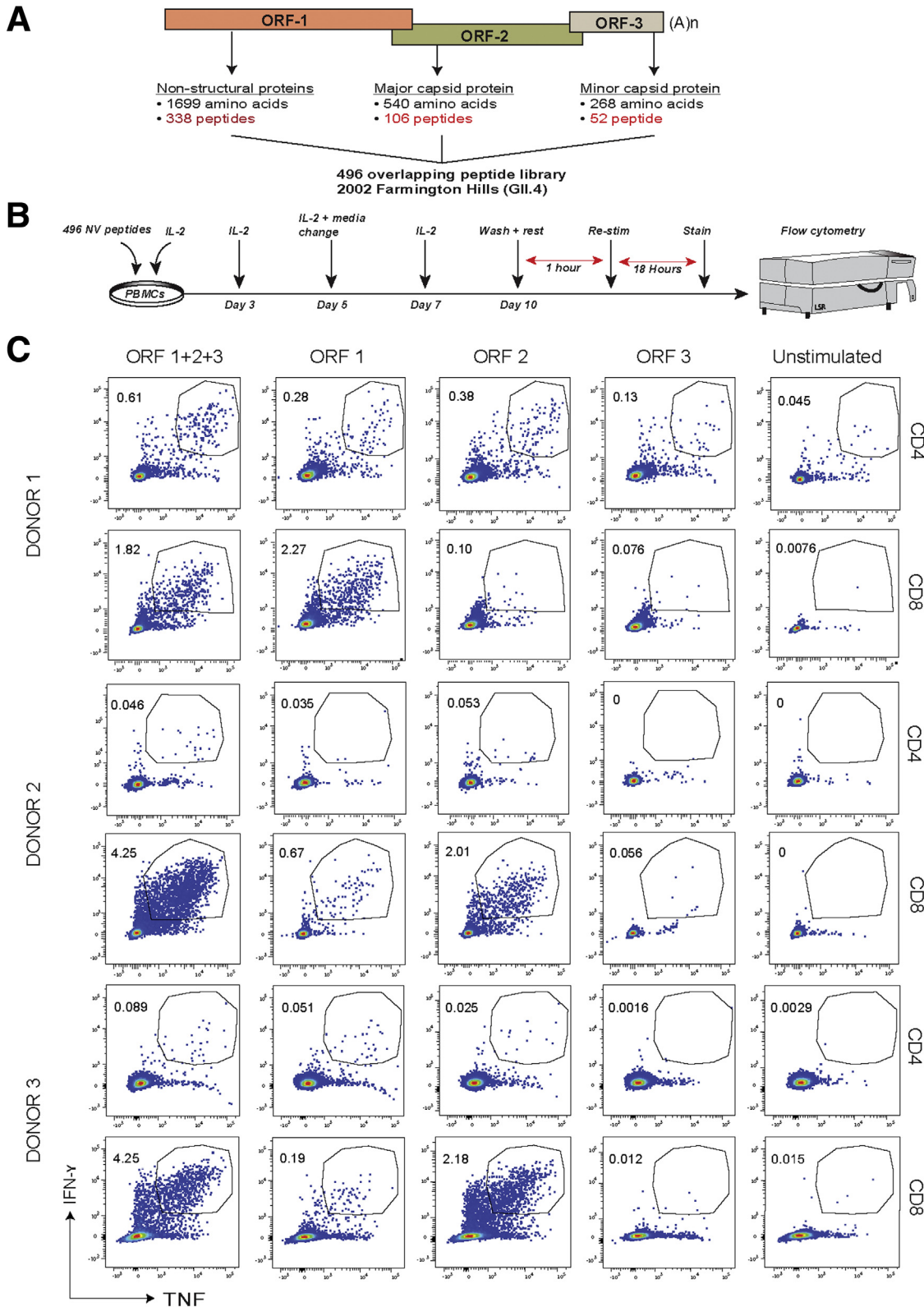
Conservation of HLA Class I Epitopes

Previously described NoV-specific T-cell responses were cross-reactive, and epitopes were conserved among genogroups.[29,30,33] We checked ORF2 and available ORF1 sequences of known epidemic and pandemic strains for conservation of the epitopes we defined. All 8 epitopes were highly conserved among GII.4 variants (Table 2), consistent with the fact that none of them fell within the hypervariable P2 capsid domain (Figure 4D). Epitopes 6, 14, and 206 were 100% conserved among all analyzed GII.4 sequences. The remaining epitopes differed by a single amino acid among variants, and in most cases these differences did not affect anchor residues. Epitope 137B, which was nondominant (Figure 4A), was the only one with variation in the C-terminal aromatic anchor (phenylalanine versus tyrosine). Interestingly, we have observed similar variation in a highly conserved MNV epitope where a Tyr→Phe change at the C-terminal anchor leads to a significantly attenuated CD8+ T-cell response.[2,45] Alignment of sequences from other GII genotypes showed that most of these 8 epitopes were broadly conserved beyond GII.4 (Table 3). As expected, there was significant divergence when epitope sequences were aligned to GI.1 variants (Table 4). Finally, a query of the basic local alignment search tool (https://blast.ncbi.nlm.nih.gov) did not find the 7 NoV epitopes within proteins from other pathogens. Thus, all 7 immunodominant CD8+ T-cell epitopes are highly conserved among GII.4 NoVs, making them valuable targets for vaccines and cell-based therapies.

Detection of Norovirus-Specific CD8+ T Cells Using HLA-Peptide Tetramers

NoV-derived T-cell epitopes have previously been described,[30,32,33] but the distribution of NoV-specific T cells in human tissues is unknown. We used HLA-peptide tetramer reagents (tetramers) to track NoV-specific CD8+ T cells in peripheral blood, lymphoid tissues, and intestinal LP. Tetramer-positive (Tet+) CD8+ T cells were readily detectable in PBMCs from the 3 HLA-matched donors (Figure 5A). Because NoV exposure is nearly universal by age 10[16] and we did not have PBMCs from young children, we used HLA-mismatched samples as negative controls for tetramer staining. Tet+ CD8+ T cells were significantly more abundant and clustered into well-defined populations in HLA-matched compared with HLA-mismatched PBMCs (Figure 5B). These data suggested that the Tet+ CD8+ T cells in HLA-matched samples were indeed NoV-specific. To further confirm the specificity of tetramer staining, we compared the abundance of Tet+ CD8+ T cells in non-stimulated PBMCs with the abundance of cytokine-producing CD8+ T cells in peptide-stimulated PBMCs from 2 donors. For this comparison, PBMCs were stimulated with all 496 NoV peptides for 18 hours without undergoing initial expansion with IL 2 (Figure 5C). Thus, we measured the "true" abundance of NoV-specific CD8+ T cells by both tetramer staining (Figure 5B) and cytokine production (Figure 5C). These analyses showed that the percentages of Tet+ (Figure 5B) and IFN-γ– and/or TNF-producing (Figure 5C) CD8+ T cells were similar (Figure 5D). For Donor 1, the abundance of NoV-specific CD8+ T cells was slightly higher when measured by tetramer staining compared with IFN-γ and TNF production (Figure 5D). This discrepancy could have been due to cell death during ex vivo stimulation or the presence of CD8+ T cells whose cytokine profiles did not include IFN-γ or TNF. Collectively, these experiments show that our tetramers captured the true abundance of epitope-specific CD8+ T cells in human peripheral blood.

Norovirus-Specific CD8+ T Cells Are Widely Distributed Across Donors and Tissues

The high degree of epitope conservation across GII NoVs (Tables 2 and 3) suggested that responses against them should be universal and not limited to individual donors. To test this hypothesis, we obtained PBMCs from 13 additional HLA-matched adult donors (Table 1) and used tetramers to screen for the presence of NoV-specific CD8+ T cells. We detected Tet+ CD8+ T cells against all 7 epitopes (Figure 6A). As expected, the abundance of NoV-specific CD8+ T cells varied by epitope and across donors, consistent with individual immune differences and/or exposure histories. These data further confirm that epitope-specific CD8+ T cells are a universal feature of the overall NoV immune response and could be an attractive target for future vaccines.

In mice, MNV-specific CD8+T cells are least abundant in the periphery and become increasingly enriched in lymphoid tissues and the intestine.[2,45] Therefore, we examined spleen (SPL) and mesenteric lymph nodes (MLN) from a deceased donor in the Human Pancreas Analysis Program who was an HLA match for epitopes 14, 106, and 32 (Figure 6B). A robust population of Tet+ CD8+ T cells was detected only with tetramer 14 in MLN and to a lesser extent SPL, suggesting that this donor either did not have CD8+ T cells specific for epitopes 32 and 106, or that such cells did not home to lymphoid tissues. Finally, we obtained duodenal tissue from 2 deceased donors who were a match for the same 3 epitopes (Figure 6C). We detected robust populations of Tet+ CD8+ T cells specific for epitopes 32 and 106, but not 14, in the LP from these donors. We did not

Figure 2. (*See previous page*). **T-cell responses after stimulation with NoV peptide libraries.** (*A*) Three peptide libraries spanning each ORF of the GII.4 2002 Farmington Hills strain were assembled. Each library consisted of 15-mer peptides overlapping neighboring peptides by 10 amino acids. A total of 496 peptides were synthesized. (*B*) Experimental design to amplify NoV-specific T-cell responses. Donor PBMCs were incubated with all 496 peptides, and responding cells were amplified over 10 days using IL2. Cells were then washed, briefly rested, and re-stimulated with individual libraries, smaller peptide pools, or single candidate peptides in the presence of brefeldin A. IFN-γ and TNF production was assessed by flow cytometry. (*C*) CD4+ and CD8+ T-cell responses in 3 donors after stimulation with full set of 496 peptides or smaller libraries spanning individual ORFs. Gated on live CD4+ or CD8+ T cells. These experiments were repeated at least 3 times.

A

	Pool 6	Pool 7	Pool 8	Pool 9	Pool 10	
Pool 1	126	127	128	129	130	Pool 11
	131	132	133	134	135	Pool 12
	136	137	138	139	140	Pool 13
	141	142	143	144	145	Pool 14
	146	147	148	149	150	Pool 15
Pool 2	151	152	153	154	155	Pool 11
	156	157	158	159	160	Pool 12
	161	162	163	164	165	Pool 13
	166	167	168	169	170	Pool 14
	171	172	173	174	175	Pool 15
Pool 3	176	177	178	179	180	Pool 11
	181	182	183	184	185	Pool 12
	186	187	188	189	190	Pool 13
	191	192	193	194	195	Pool 14
	196	197	198	199	200	Pool 15
Pool 4	201	202	203	204	205	Pool 11
	206	207	208	209	210	Pool 12
	211	212	213	214	215	Pool 13
	216	217	218	219	220	Pool 14
	221	222	223	224	225	Pool 15
Pool 5	226	227	228	229	230	Pool 11
	231	232	233	234	235	Pool 12
	236	237	238	239	240	Pool 13
	241	242	243	244	245	Pool 14
	246	247	248	249	250	Pool 15

B

C

D

Peptide 137 : RASGLLHERLDEFEL

Epitope	Sequence	Favoured HLA	IEDB Percentile rank
137 A	LLHERLDEF	HLA-C*03:02	0.54
137 B	HERLDEFEL	HLA-B*40:01	0.54

Figure 3. Peptide library screening strategy. (*A*) Overlapping pools of 20–25 peptides were assembled in 3-dimensional matrix arrangement. In this example, peptide 137 was included in pools 1, 7, and 13. (*B*) Donor PBMCs were stimulated with each of the 15 pools, and cytokine responses were detected with pools 1, 7, and 13, suggesting that peptide 137 contained an immunodominant epitope. (*C*) PBMCs from the same donor were then stimulated with peptide 137, confirming a robust response. (*D*) Analysis of peptide 137 using the IEDB (https://www.iedb.org/) uncovered 2 potential HLA-restricted epitopes within the 15-mer sequence that were subsequently tested (Figure 4*A*).
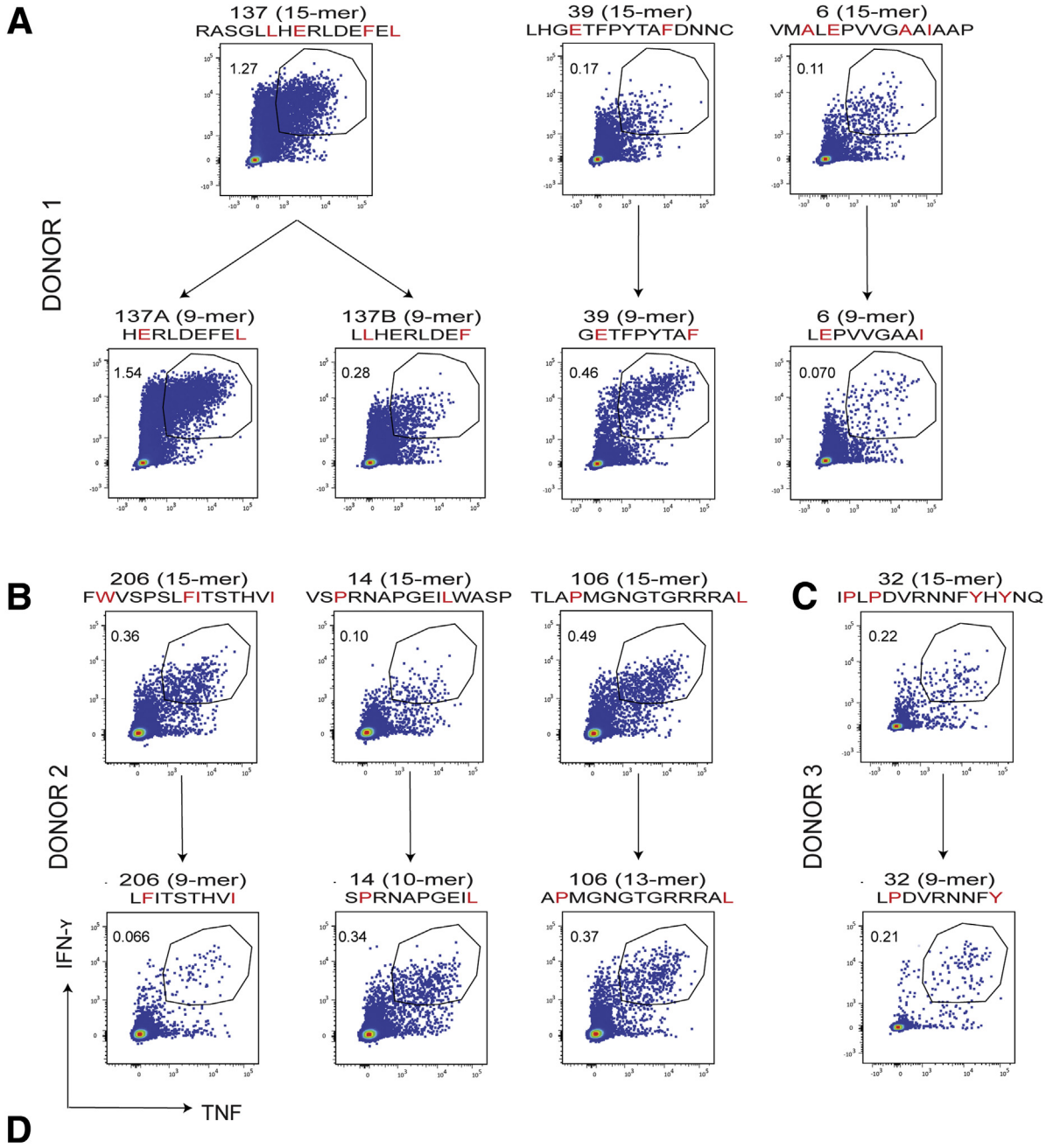
Figure 4. Defining HLA-restricted immunodominant HLA class I. Candidate 15-mer peptides were identified as described in Figure 3. Next, shorter peptides were generated from 15-mers on the basis of donor HLA types and predicted anchor residues (https://www.iedb.org/ and http://www.cbs.dtu.dk/services/NetMHCpan/). These shorter candidate epitopes were tested using the method shown in Figure 2. Anchor residues are shown in *red*. (*A–C*) Epitopes deriving from 15-mer library peptides for Donors 1, 2, and 3. (*D*) Summary of epitope sequences, location, and HLA restriction.

Donor	Peptide	Length	Sequence (Anchors)	ORF	Position in ORF	Location	Predicted HLA	IEDB Percentile Rank	NetMHCpan Prediction
1	137A	9	HERLDEFEL	1	687-695	NTPase	HLA-B*40:01	0.54	Strong Binder
1	137B	9	LLHERLDEF	1	685-693	NTPase	HLA-C*03:02	0.54	Strong Binder
1	39	9	GETFPYTAF	1	193-201	p48	HLA-B*40:01	0.42	Strong Binder
1	6	9	LEPVVGAAI	2	29-37	N-terminal domain	HLA-B*40:01	0.6	Strong Binder
2	206	9	LFITSTHVI	1	1032-1040	Vpg	HLA-A*24:02	0.99	Weak Binder
2	14	10	SPRNAPGEIL	2	67-76	S domain	HLA-B*07:02	0.08	Strong Binder
2	106	13	APMGNGTGRRRAL	2	528-540	P1	HLA-B*07:02	0.02	Strong Binder
3	32	9	LPDVRNNFY	2	158-166	S domain	HLA-B*35:01	1.1	Strong Binder

Table 2. Conservation of CD8+ T-Cell Epitopes Across GII.4 NoV Strains

Epitope (HLA)	GII.4 strain	%Similarity	Sequence	Epitope (HLA)	GII.4 Strain	%Similarity	Sequence
137A (B*40:01)	Farmington_Hills_2002	100	H *E* R L D E F E *L*	137B (C*03:02)	Farmington_Hills_2002	100	L *L* H E R L D E *F*
	New_Orleans_2009	100	H E R L D E F E L		New_Orleans_2009	100	L L H E R L D E F
	Hunter_2004	100	H E R L D E F E L		Hunter_2004	100	L L H E R L D E F
	Oxford_2002	100	H E R L D E F E L		Oxford_2002	100	L L H E R L D E F
	Sydney_2012	88.89	H E R L D E **Y** E L		Sydney_2012	88.89	L L H E R L D E **Y**
	Lorsdale_1993	88.89	H E R L D E **Y** E L		Lorsdale_1993	88.89	L L H E R L D E **Y**
	Camberwell_1987	88.89	H E R L D E **Y** E L		Camberwell_1987	88.89	L L H E R L D E **Y**
39 (B*40:01)	Farmington_Hills_2002	100	G *E* T F P Y T A *F*	206 (A*24:02)	Farmington_Hills_2002	100	L *F* I T S T H V *I*
	New_Orleans_2009	100	G E T F P Y T A F		New_Orleans_2009	100	L F I T S T H V I
	Hunter_2004	100	G E T F P Y T A F		Hunter_2004	100	L F I T S T H V I
	Oxford_2002	100	G E T F P Y T A F		Oxford_2002	100	L F I T S T H V I
	Sydney_2012	88.89	G E **S** F P Y T A F		Sydney_2012	100	L F I T S T H V I
	Lorsdale_1993	88.89	G E **S** F P Y T A F		Lorsdale_1993	100	L F I T S T H V I
	Camberwell_1987	88.89	G E **S** F P Y T A F		Camberwell_1987	100	L F I T S T H V I
6 (B*40:01)	Farmington_Hills_2002	100	L *E* P V V G A A *I*	14 (B*07:02)	Farmington_Hills_2002	100	S *P* R N A P G E I *L*
	Camberwell_1987	100	L E P V V G A A I		Camberwell_1987	100	S P R N A P G E I L
	Lorsdale_1993	100	L E P V V G A A I		Lorsdale_1993	100	S P R N A P G E I L
	Grimsby_1995	100	L E P V V G A A I		Grimsby_1995	100	S P R N A P G E I L
	Dresden_1997	100	L E P V V G A A I		Dresden_1997	100	S P R N A P G E I L
	Bochum_1997	100	L E P V V G A A I		Bochum_1997	100	S P R N A P G E I L
	Oxford_2002	100	L E P V V G A A I		Oxford_2002	100	S P R N A P G E I L
	Hunter_2004	100	L E P V V G A A I		Hunter_2004	100	S P R N A P G E I L
	Den_Haag_2006	100	L E P V V G A A I		Den_Haag_2006	100	S P R N A P G E I L
	Yerseke_2006	100	L E P V V G A A I		Yerseke_2006	100	S P R N A P G E I L
	Apeldoorn_2007	100	L E P V V G A A I		Apeldoorn_2007	100	S P R N A P G E I L
	New_Orleans_2009	100	L E P V V G A A I		New_Orleans_2009	100	S P R N A P G E I L
	Sydney_2012	100	L E P V V G A A I		Sydney_2012	100	S P R N A P G E I L
32 (B*35:01)	Farmington_Hills_2002	100	L *P* D V R N N F *Y*	106 (B*07:02)	Farmington_Hills_2002	100	A *P* M G N G T G R R A *L*
	Camberwell_1987	100	L P D V R N N F Y		Camberwell_1987	100	A P M G N G T G R R A L
	Lorsdale_1993	100	L P D V R N N F Y		Lorsdale_1993	100	A P M G N G T G R R A L
	Grimsby_1995	100	L P D V R N N F Y		Grimsby_1995	92.31	A P M G N G **A** G R R A L
	Dresden_1997	100	L P D V R N N F Y		Dresden_1997	92.31	A P M G N G **A** G R R A L
	Oxford_2002	100	L P D V R N N F Y		Oxford_2002	100	A P M G N G T G R R A L
	Den_Haag_2006	100	L P D V R N N F Y		Den_Haag_2006	100	A P M G N G T G R R A L
	Yerseke_2006	100	L P D V R N N F Y		Yerseke_2006	100	A P M G N G T G R R A L
	Apeldoorn_2007	100	L P D V R N N F Y		Apeldoorn_2007	100	A P M G N G T G R R A L

Table 2. Continued

Epitope (HLA)	GII.4 strain	%Similarity	Sequence	Epitope (HLA)	GII.4 Strain	%Similarity	Sequence
	New_Orleans_2009	100	L P D V R N N F Y		New_Orleans_2009	100	A P M G N G T G R R R A L
	Sydney_2012	100	L P D V R N N F Y		Sydney_2012	100	A P M G N G T G R R R A L
	Bochum_1997	88.89	L P D **G** R N N F Y		Bochum_1997	92.31	A P M G N G **A** G R R R A L
	Hunter_2004	88.89	L P D V R N N **L** Y		Hunter_2004	92.31	A P M G N G **A** G R R R A L

NOTE. Alignments to other GII sequences are shown in Table 3. Epitopes were aligned to available sequences for several GII.4 epidemic and pandemic strains. For each epitope, the sequence identified from the Farmington Hills strain is shown at the top with anchor residues in italics. Bold font indicates variable residues. Note that complete ORF1 and ORF2 sequences were not available for all strains; thus not every epitope could be compared across all strains.

have a full set of peripheral, lymphoid, and intestinal samples from the same donor and thus could not compare the anatomic distribution of individual epitope-specific T cell clones within the same subject. However, our observations were broadly consistent with data from the mouse model, where MNV-specific T cells are most abundant in intestinal tissues.[2,45] Our findings also suggest that CD8^{+} T cells with different epitope specificity may have distinct tissue distribution.

Norovirus-Specific CD8^{+} T Cells Have Distinct Phenotypes Based on Tissue Distribution

T_{RM} reside permanently within organs such as the intestine, where they act as "first responders" during pathogen reexposure.[49] T_{RM} must therefore balance inflammatory and regulatory pathways to provide sufficient protection from pathogens, while minimizing local tissue damage.[50–52] In line with these requirements, we have shown that MNV-specific CD8^{+} T_{RM} follow a unique differentiation program and retain both effector and exhaustion features.[2] To explore this question in humans, we analyzed Tet[+] PBMCs and lamina LP mononuclear cells (LPMCs) for markers of memory differentiation, tissue residence, exhaustion, cytotoxicity, and proliferation (Figure 7). Tet^{+} CD8^{+} PBMCs were mainly CD45RA⁻CCR7⁻ or CD45RA⁻CCR7⁺, consistent with effector memory (T_{EM}) or central memory (T_{CM}) lineages, respectively (Figure 7A, column 1). T_{EM} cells re-expressing CD45RA (T_{EMRA}) were detected only for epitope 39. As expected, most Tet^{+} CD8^{+} T cells in the periphery did not express the key marker for tissue residence, CD69. However, some Tet^{+} CD8^{+} T cells expressed the α integrin CD103, suggesting that they could be retained upon recruitment to intestinal tissues (Figure 7A, column 2). These observations were reminiscent of findings from the mouse model, where both CD103[HI] and CD103[LOW] MNV-specific T-cell subsets develop.[2] Tet^{+} CD8^{+} PBMCs did not up-regulate the immunoregulatory marker PD-1, which is associated with T-cell exhaustion, although some of them expressed the transcription factor EOMES, which can be associated with either exhaustion or T_{CM} (Figure 7A, column 3). Consistent with the fact that our donors were not acutely infected with NoV, Tet^{+} CD8^{+} PBMCs were not actively proliferating as measured by Ki67 staining. Most Tet^{+} CD8^{+} PBMCs were also low for granzyme B, consistent with T_{CM} lineage.[53] (Figure 7A, column 4). Only epitope 39–specific CD8^{+} T cells showed significant granzyme B expression, and most of these cytotoxic cells came from the T_{EM} and T_{EMRA} pools (data not shown).

In contrast to PBMCs, Tet^{+} CD8^{+} T cells in the intestinal LP were mostly T_{EM}, and many of them expressed CD69, consistent with tissue residence (Figure 7B). As in the periphery and consistent with findings from the MNV model, both CD103^{+} and CD103⁻ Tet^{+} CD8^{+} T cells were present in the intestine[2] (Figure 7B, column 2). NoV-specific CD8^{+} T cells did not express PD-1 or EOMES, suggesting that they were not exhausted (Figure 7B,

Table 3. Conservation of CD8$^+$ T-Cell Epitopes Across GII NoV Strains

137A (B*40:01)	Strain	%									
	Farmington_Hills_2002	100	H	*E*	R	L	D	E	F	E	*L*
	GII.1/Hawaii	89	H	E	R	L	D	E	**Y**	E	L
	GII.22/Yuri	89	H	E	R	L	D	E	F	**D**	L
	GII.24/Loreto1972	89	H	E	R	L	D	E	F	**D**	L
	GII.26/Leon4509	89	H	E	R	L	D	E	F	**D**	L
	GII.27/Loreto0959	89	H	E	R	L	D	E	F	**D**	L
	GII.NA1/Loreto1257	89	H	E	R	L	D	E	F	**D**	L
	GII.NA2/PNV06929	89	H	E	R	L	D	E	F	**D**	L

137B (C*03:02)	Strain	%									
	Farmington_Hills_2002	100	L	*L*	H	E	R	L	D	E	*F*
	GII.1/Hawaii	89	L	L	H	E	R	L	D	E	**Y**
	GII.22/Yuri	100	L	L	H	E	R	L	D	E	F
	GII.24/Loreto1972	100	L	L	H	E	R	L	D	E	F
	GII.26/Leon4509	100	L	L	H	E	R	L	D	E	F
	GII.27/Loreto0959	100	L	L	H	E	R	L	D	E	F
	GII.NA1/Loreto1257	100	L	L	H	E	R	L	D	E	F
	GII.NA2/PNV06929	100	L	L	H	E	R	L	D	E	F

39 (B*40:01)	Strain	%									
	Farmington_Hills_2002	100	G	*E*	T	F	P	Y	T	A	*F*
	GII.1/Hawaii	89	G	E	**S**	F	P	Y	T	A	F
	GII.22/Yuri	89	G	E	**S**	F	P	Y	T	A	F
	GII.24/Loreto1972	100	G	E	T	F	P	Y	T	A	F
	GII.26/Leon4509	100	G	E	T	F	P	Y	T	A	F
	GII.27/Loreto0959	89	G	E	**S**	F	P	Y	T	A	F
	GII.NA1/Loreto1257	89	G	E	**S**	F	P	Y	T	A	F
	GII.NA2/PNV06929	89	G	E	**S**	F	P	Y	T	A	F

206 (A*24:02)	Strain	%								
	Farmington_Hills_2002	100	L	*F*	I	T	S	T	H	V	*I*
	GII.1/Hawaii	100	L	F	I	T	S	T	H	V	I
	GII.22/Yuri	100	L	F	I	T	S	T	H	V	I
	GII.24/Loreto1972	100	L	F	I	T	S	T	H	V	I
	GII.26/Leon4509	100	L	F	I	T	S	T	H	V	I
	GII.27/Loreto0959	100	L	F	I	T	S	T	H	V	I
	GII.NA1/Loreto1257	100	L	F	I	T	S	T	H	V	I
	GII.NA2/PNV06929	89	L	F	I	T	S	T	H	V	**V**

6 (B*40:01)	Strain	%								
	Farmington_Hills_2002	100	L	*E*	P	V	V	G	A	A	*I*
	GII.1/Hawaii	78	L	E	P	V	**A**	G	A	**S**	I
	GII.2/Chapel hill	78	L	E	P	V	**A**	G	A	A	**L**
	GII.3/TV24	78	L	E	P	V	**A**	G	**S**	A	I
	GII.5/Hillingdon	78	L	E	P	V	V	G	A	**S**	**L**
	GII.6/Seacroft	89	L	E	P	V	V	G	A	**S**	I
	GII.7/Leeds	67	L	E	P	V	**A**	G	A	**S**	**L**
	GII.8/Amsterdam	67	**I**	E	P	V	**A**	G	A	**S**	**L**
	GII.9/VA97207	67	**I**	E	P	V	**A**	G	A	**S**	I
	GII.10/Erfurt546	67	L	E	P	V	**A**	G	A	**S**	**L**
	GII.11/Sw918	78	L	E	P	V	V	G	A	**P**	**L**
	GII.12/Wortley	78	L	E	P	V	**A**	G	A	**S**	I
	GII.13/Fayetteville	78	L	E	P	V	**A**	G	A	**S**	I
	GII.14/M7	78	L	E	P	V	**A**	G	A	**S**	I
	GII.16/Tiffin	78	L	E	P	V	**A**	G	A	**S**	I
	GII.17/CS-E1	89	L	E	P	V	**A**	G	A	A	I
	GII.18/OH-QW101	78	L	E	P	V	**A**	G	A	A	**L**
	GII.19/OH-QW170	78	L	E	P	V	V	G	A	**P**	**L**
	GII.20/Luckenwalde591	89	L	E	P	V	**A**	G	A	A	I
	GII.21/IF1998	89	L	E	P	V	**A**	G	A	A	I
	GII.22/Yuri	78	L	E	P	V	**A**	G	**G**	A	I
	GII.23/Loreto1847	78	L	E	P	V	**A**	G	**G**	A	I

14 (B*07:02)	Strain	%									
	Farmington_Hills_2002	100	S	*P*	R	N	A	P	G	E	I	*L*
	GII.1/Hawaii	90	S	P	R	N	**S**	P	G	E	I	L
	GII.2/Chapel hill	90	S	P	R	N	A	P	G	E	**V**	L
	GII.3/TV24	80	S	P	R	N	**S**	P	G	E	**V**	L
	GII.5/Hillingdon	80	S	P	**K**	N	**S**	P	G	E	I	L
	GII.6/Seacroft	80	S	P	R	N	**S**	P	G	E	**M**	L
	GII.7/Leeds	90	S	P	R	N	**S**	P	G	E	I	L
	GII.8/Amsterdam	90	S	P	R	N	A	P	G	E	**F**	L
	GII.9/VA97207	90	S	P	R	N	A	P	G	E	**F**	L
	GII.10/Erfurt546	80	S	P	R	N	**S**	P	G	E	**V**	L
	GII.11/Sw918	100	S	P	R	N	A	P	G	E	I	L
	GII.12/Wortley	80	S	P	R	N	**S**	P	G	E	**V**	L
	GII.13/Fayetteville	90	S	P	R	N	**S**	P	G	E	I	L
	GII.14/M7	80	S	P	R	N	**S**	P	G	E	**L**	L
	GII.16/Tiffin	90	S	P	R	N	**S**	P	G	E	I	L
	GII.17/CS-E1	90	S	P	R	N	**S**	P	G	E	I	L
	GII.18/OH-QW101	80	S	P	R	N	**S**	P	G	E	**V**	L
	GII.19/OH-QW170	100	S	P	R	N	A	P	G	E	I	L
	GII.20/Luckenwalde591	90	S	P	R	N	A	P	G	E	**V**	L
	GII.21/IF1998	90	S	P	R	N	**S**	P	G	E	I	L
	GII.22/Yuri	90	S	P	R	N	**S**	P	G	E	I	L
	GII.23/Loreto1847	90	S	P	R	N	**S**	P	G	E	I	L

Table 3. Continued

Epitope	Strain	Pos	1	2	3	4	5	6	7	8	9
	GII.24/Loreto1972	78	L	E	P	V	**A**	G	**G**	A	I
	GII.25/Beijing53931	78	L	E	P	V	**A**	G	**G**	A	I
32 (B*35:01)	Farmington_Hills_2002	100	L	*P*	D	V	R	N	N	F	*Y*
	GII.1/Hawaii	89	L	P	D	V	R	N	N	F	**F**
	GII.2/Chapel hill	89	L	P	D	V	R	N	N	F	**F**
	GII.3/TV24	78	**M**	P	D	V	R	N	N	F	**F**
	GII.5/Hillingdon	44	**M**	P	D	V	R	**S**	**T**	**L**	**F**
	GII.6/Seacroft	67	L	P	D	**I**	R	N	**R**	F	**F**
	GII.7/Leeds	56	**M**	P	D	**I**	**K**	N	N	F	**F**
	GII.8/Amsterdam	56	**M**	P	D	**I**	R	N	**T**	F	**F**
	GII.9/VA97207	56	**M**	P	D	**I**	R	N	**T**	F	**F**
	GII.10/Erfurt546	56	**M**	P	D	**I**	R	N	**S**	F	**F**
	GII.11/Sw918	44	**M**	P	D	**I**	R	N	**K**	**L**	**F**
	GII.12/Wortley	67	**F**	P	D	V	R	N	**S**	F	**F**
	GII.13/Fayetteville	89	L	P	D	V	R	N	**V**	F	Y
	GII.14/M7	67	**M**	P	D	**I**	R	N	**V**	F	Y
	GII.16/Tiffin	89	L	P	D	V	R	N	N	F	**F**
	GII.17/CS-E1	78	L	P	D	V	R	N	**T**	F	**F**
	GII.18/OH-QW101	78	**M**	P	D	V	R	N	N	F	**F**
	GII.19/OH-QW170	56	**M**	P	D	V	R	N	**R**	**L**	**F**
	GII.20/Luckenwalde591	100	L	P	D	V	R	N	N	F	Y
	GII.21/IF1998	89	L	P	D	V	R	N	**V**	F	Y
	GII.22/Yuri	67	**M**	P	D	V	R	N	**Q**	F	**F**
	GII.23/Loreto1847	78	**V**	P	D	V	R	N	N	F	**F**
	GII.24/Loreto1972	89	L	P	D	V	R	N	**S**	F	Y
	GII.25/Beijing53931	78	L	P	D	V	R	N	**Q**	F	**F**

Epitope	Strain	Pos	1	2	3	4	5	6	7	8	9	10	11	12
	GII.24/Loreto1972	80	S	P	R	N	**S**	P	G	E	**V**	L		
	GII.25/Beijing53931	80	S	P	R	N	**S**	P	G	E	**V**	L		
106 (B*07:02)	Farmington_Hills_2002	100	A	*P*	M	G	N	G	**T**	G	R	R	A	*L*
	GII.1/Hawaii	69	A	P	M	G	**T**	G	**N**	G	R	R	**V**	**Q**
	GII.2/Chapel Hill	69	A	P	M	G	**T**	G	**N**	G	R	R	**V**	**Q**
	GII.3/TV24	69	A	P	M	G	**T**	G	**N**	G	R	R	**I**	**Q**
	GII.5/Hillingdon	69	A	P	M	G	**T**	G	**N**	G	R	R	**F**	**Q**
	GII.6/Seacroft	77	A	P	M	G	**S**	G	**Q**	G	R	R	A	**Q**
	GII.7/Leeds	62	A	P	**V**	G	**T**	G	**N**	G	R	R	**V**	**Q**
	GII.8/Amsterdam	62	A	P	**V**	G	**T**	G	**S**	G	R	R	**V**	**Q**
	GII.9/VA97207	62	A	P	**V**	G	**T**	G	**S**	G	R	R	**I**	**Q**
	GII.10/Erfurt546	77	A	P	M	G	N	G	**S**	G	R	R	**M**	**Q**
	GII.11/Sw918	85	A	P	M	G	N	G	**S**	G	R	R	A	**R**
	GII.12/Wortley	69	A	P	M	G	**T**	G	**N**	G	R	R	**V**	**Q**
	GII.13/Fayetteville	69	A	P	M	G	**T**	G	**N**	G	R	R	**I**	**Q**
	GII.14/M7	62	A	P	**V**	G	**T**	G	**S**	G	R	R	**I**	**Q**
	GII.16/Tiffin	69	A	P	M	G	**T**	G	**N**	G	R	R	**M**	**Q**
	GII.17/CS-E1	69	A	P	M	G	**T**	G	**N**	G	R	R	**V**	**Q**
	GII.18/OH-QW101	77	A	P	M	G	**S**	G	**T**	G	R	R	**N**	**Q**
	GII.19/OH-QW170	77	A	P	M	G	N	G	**S**	G	R	R	**V**	**Y**
	GII.20/Luckenwalde591	38	A	P	M	G	**T**	G	**R**	A	E	E	**I**	**Q**
	GII.21/IF1998	69	A	P	M	G	**T**	G	**N**	G	R	R	**I**	**Q**
	GII.22/Yuri	69	A	P	M	G	**N**	G	**N**	G	R	R	**I**	**Q**
	GII.23/Loreto1847	69	A	P	M	G	**T**	G	**N**	G	R	R	**I**	**Q**
	GII.24/Loreto1972	69	A	P	M	G	**T**	G	**N**	G	R	R	**I**	**Q**
	GII.25/Beijing53931	77	A	P	M	G	**N**	G	**N**	G	R	R	**V**	**Q**

NOTE. Alignments to GII.4 sequences are shown in Table 2. Epitopes were aligned to representative GII sequences. For each epitope, the sequence identified from the Farmington Hills strain is shown at the top with anchor residues in italics. Bold font indicates variable residues. Note that complete ORF1 and ORF2 sequences were not available for all strains; thus not every epitope could be compared across all strains.

Table 4. Alignment of CD8$^+$ T-Cell Epitopes to GI.1 NoV Sequences

Epitope (HLA)	GI strain	% Similarity	Sequence									
137A (B*40:01)	Farmington_Hills_2002	100	H	*E*	R	L	D	E	F	E	*L*	
	GI.I/Hu/CHA9A004/USA	66.60	**M**	E	R	**Q**	D	E	F	**Q**	L	
	GI.I/Hu/Norwalk	66.60	**M**	E	R	**Q**	D	E	F	**Q**	L	
137B (C*03:02)	Farmington_Hills_2002	100	L	*L*	H	E	R	L	D	E	*F*	
	GI.I/Hu/CHA9A004/USA	66.60	L	**T**	**M**	E	R	**Q**	D	E	F	
	GI.I/Hu/Norwalk	66.60	L	**T**	**M**	E	R	**Q**	D	E	F	
206 (A*24:02)	Farmington_Hills_2002	100	L	*F*	I	T	S	T	H	V	*I*	
	GI.I/Hu/CHA9A004/USA	66.60	**V**	F	I	T	**T**	T	H	V	**V**	
	GI.I/Hu/Norwalk	66.60	**V**	F	I	T	**T**	T	H	V	**V**	
32 (B*35:01)	Farmington_Hills_2002	100	L	*P*	D	V	R	N	N	F	*Y*	
	GI.I/Hu/CHA9A004/USA	44.40	L	**E**	D	V	R	N	**V**	**L**	**F**	
	GI.I/Hu/Norwalk	44.40	L	**E**	D	V	R	N	**V**	**L**	**F**	
	GI.1/Hu/SRSVKY8989	44.40	L	**E**	D	V	R	N	**V**	**L**	**F**	
14 (B*07:02)	Farmington_Hills_2002	100	S	*P*	R	N	A	P	G	E	I	*L*
	GI.I/Hu/CHA9A004/USA	60	S	P	**N**	N	**T**	P	G	**D**	**V**	L
	GI.I/Hu/Norwalk	60	S	P	**N**	N	**T**	P	G	**D**	**V**	L
	GI.1/Hu/SRSVKY8989	60	S	P	**N**	N	**T**	P	G	**D**	**V**	L

NOTE. Epitopes were aligned to available sequences from GI strains. For each epitope, the sequence identified from the Farmington Hills strain is shown at the top with anchor residues in italics. Bold font indicates variable residues. Only conserved epitopes are shown.

column 3). Moreover, a significant proportion of the epitope 106–specific CD8$^+$ T cells produced granzyme B (Figure 7*B*, column 4), and this cytotoxic subset was CD69$^+$ CD103$^+$, indicating they were T$_{RM}$ (Figure 7*C*). Collectively, these experiments begin to define NoV-specific T-cell immunity directly in humans. Our data suggest that Tet$^+$ CD8$^+$ T cells are broadly distributed across tissues and display a range of phenotypic and functional properties.

Conclusions

NoVs are the leading cause of food-borne illness globally[54] and have been designated a priority pathogen for vaccine development by the World Health Organization.[55] Although several clinical trials are currently underway,[5] significant challenges continue to hamper the development of an effective NoV vaccine. First, GII.4 NoVs continuously evolve to escape preexisting neutralizing antibodies, as evidenced by the emergence of new pandemic variants.[12] Thus, antibody-based vaccines will likely have limited cross-strain breadth and require periodic reformulation. Second, antibody-mediated protection alone may not be sufficient, and other correlates of NoV immunity, including cellular responses, must be elucidated. Conversely, host-NoV interactions that enable immune evasion and long-term persistence are similarly unclear. Third, propagating human NoVs in cell culture remains difficult despite recent advances in this area,[56,57] and these systems cannot fully recapitulate the complex immune environment of the intestine. Our findings and the reagents we have developed help address these limitations by defining conserved T-cell epitopes and enabling the study of NoV-specific T cells directly in human tissues.

Current NoV vaccine candidates incorporate GI.1 and GII.4 sequences, and readouts of immunogenicity are primarily based on antibody titers.[5] The ability to also measure T-cell responses could enable a more comprehensive assessment of NoV immunity, particularly when coupled to post-vaccination challenge outcomes. Whereas neutralizing antibodies against GII.4 viruses target the viral capsid and are mostly strain-specific, the T-cell epitopes we describe are highly conserved and could generate broadly reactive responses across GII.4 (Figure 4). Importantly, VLPs, which are devoid of nonstructural proteins and do not replicate intracellularly, may not be able to take advantage of these CD8$^+$ T-cell epitopes. Future studies will have to determine whether incorporating specific T-cell epitopes into live or mRNA vaccine formulations can boost overall protection and/or mitigate disease severity.

Another therapeutic application of our findings could be in T cell–based therapies of chronic NoV infection, as recently proposed by Hanajiri et al[33] and used in other settings.[58,59] Tetramers can simplify the purification of donor NoV-specific T cells and their subsequent tracking in immunocompromised recipients. In this regard, our findings could be especially valuable, because they add to the short list of known human HLA class I restricted NoV epitopes.[32,33] Although Hanajiri et al used a GII.4 peptide library based on the Sydney_2012 strain of similar design to ours (15-mers, overlapping by 10 amino acids), their findings were biased in favor of HLA class II restricted epitopes. Differences in donor exposures and/or HLA types between the 2 studies might account for these discrepancies. For example, of the 3 CD8$^+$ T-cell epitopes described by Hanajiri et al, only one was restricted to an HLA type (B*35:01) that
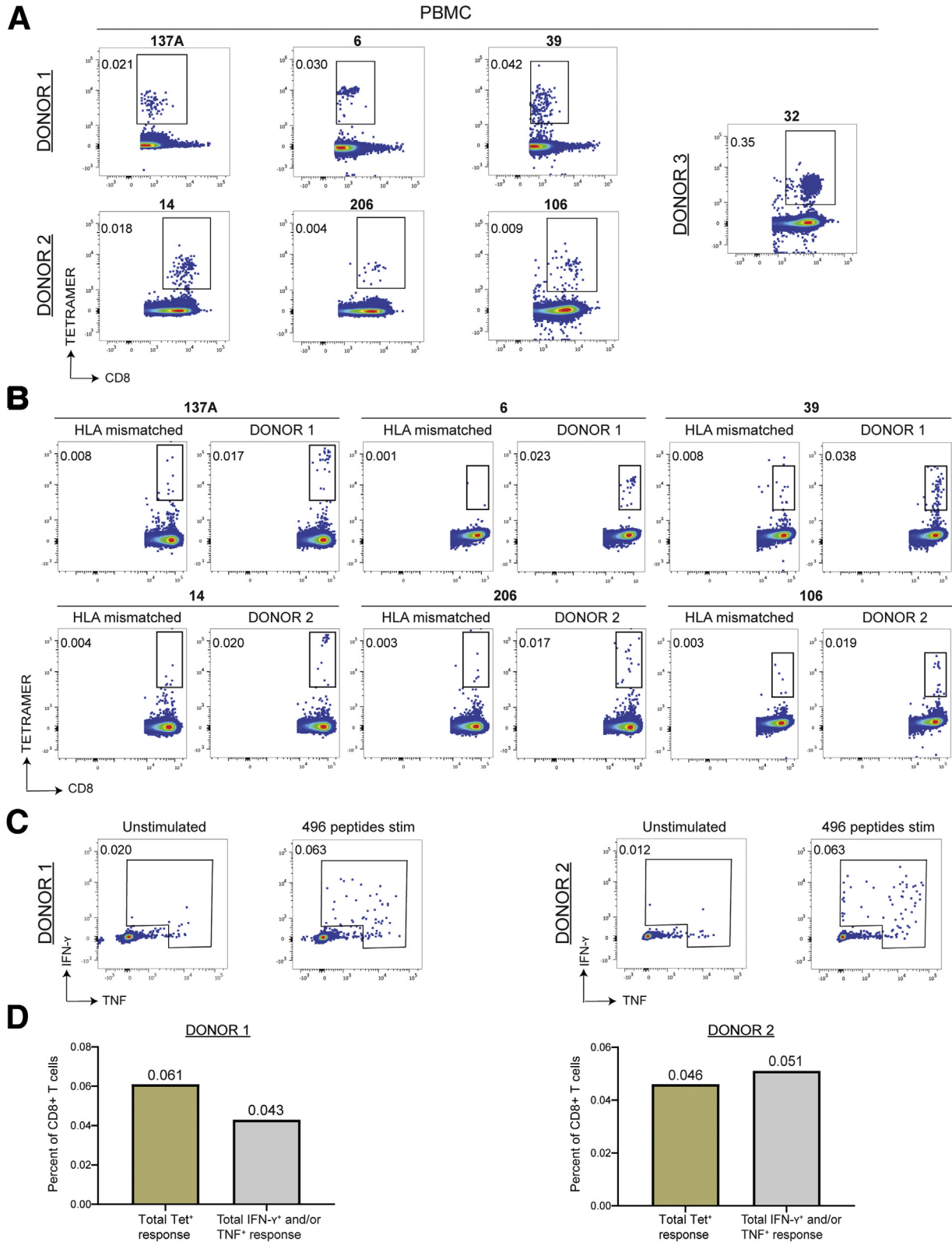
Figure 5. Detection of Nov-specific CD8$^+$ T cells using HLA-peptide tetramers. (*A*) PBMCs from 3 donors were stained with HLA-matched tetramers to detect NoV-specific CD8$^+$ T cells. Representative of 3 independent experiments. (*B*) To confirm tetramer specificity, each tetramer was used to stain HLA-matched and HLA-mismatched PBMCs. Total abundance of Tet$^+$ cells for each donor was calculated by adding the percentage of Tet$^+$ cells from HLA-matched samples and subtracting nonspecific staining from HLA-mismatched samples. Donor 1: (0.017 + 0.023 + 0.038) − (0.008 + 0.001 + 0.008) = 0.061. Donor 2: (0.020 + 0.017 + 0.019) − (0.004 + 0.003 + 0.003) = 0.046. (*C*) PBMCs from Donors 1 and 2 were stimulated for 18 hours with all 496 NoV peptides (without addition of IL2), and IFN-γ and TNF responses were measured by flow cytometry. Unstimulated PBMCs were analyzed in parallel, and the nonspecific cytokine signal was subtracted from stimulated samples. Donor 1: (0.063 − 0.020) = 0.043. Donor 2: (0.063 − 0.012) = 0.051. (*D*) Summary of data from (*B*) and (*C*).
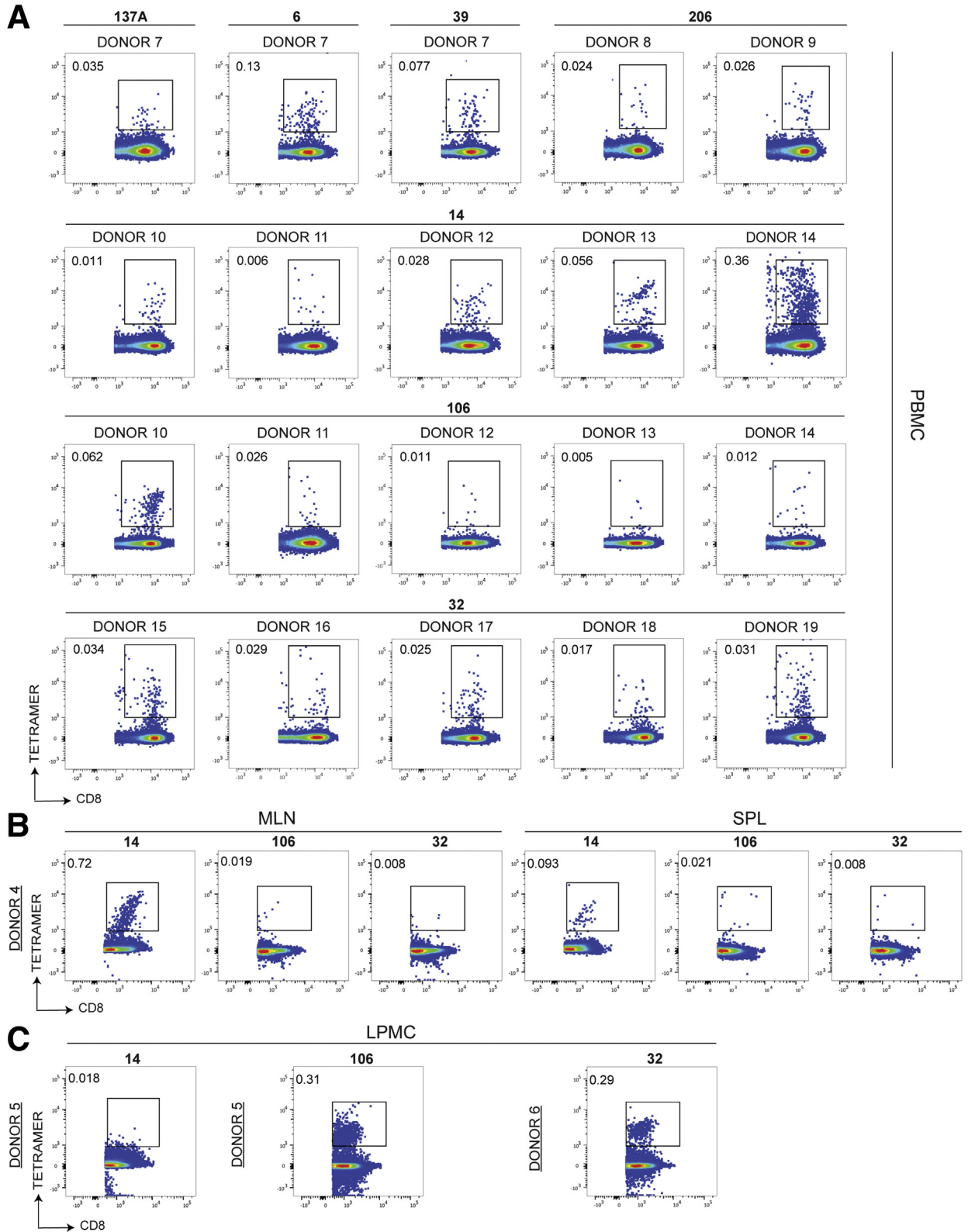
Figure 6. NoV-specific CD8$^+$ T cells are distributed broadly across donors and tissues. (*A*) PBMCs from 13 additional HLA-typed adult donors were stained with tetramers. (*B*) Cells from MLN and SPL from a deceased donor (Donor 4) who was an HLA match for epitopes 14, 106, and 32 were stained with tetramers. (*C*) LPMCs from 2 different deceased donors (Donors 5 and 6) whose HLAs were a match for epitopes 14, 106, and 32 were stained with tetramers. Staining for (*B*) and (*C*) could only be done once because of limited samples. Gated on live CD8$^+$ T cells.
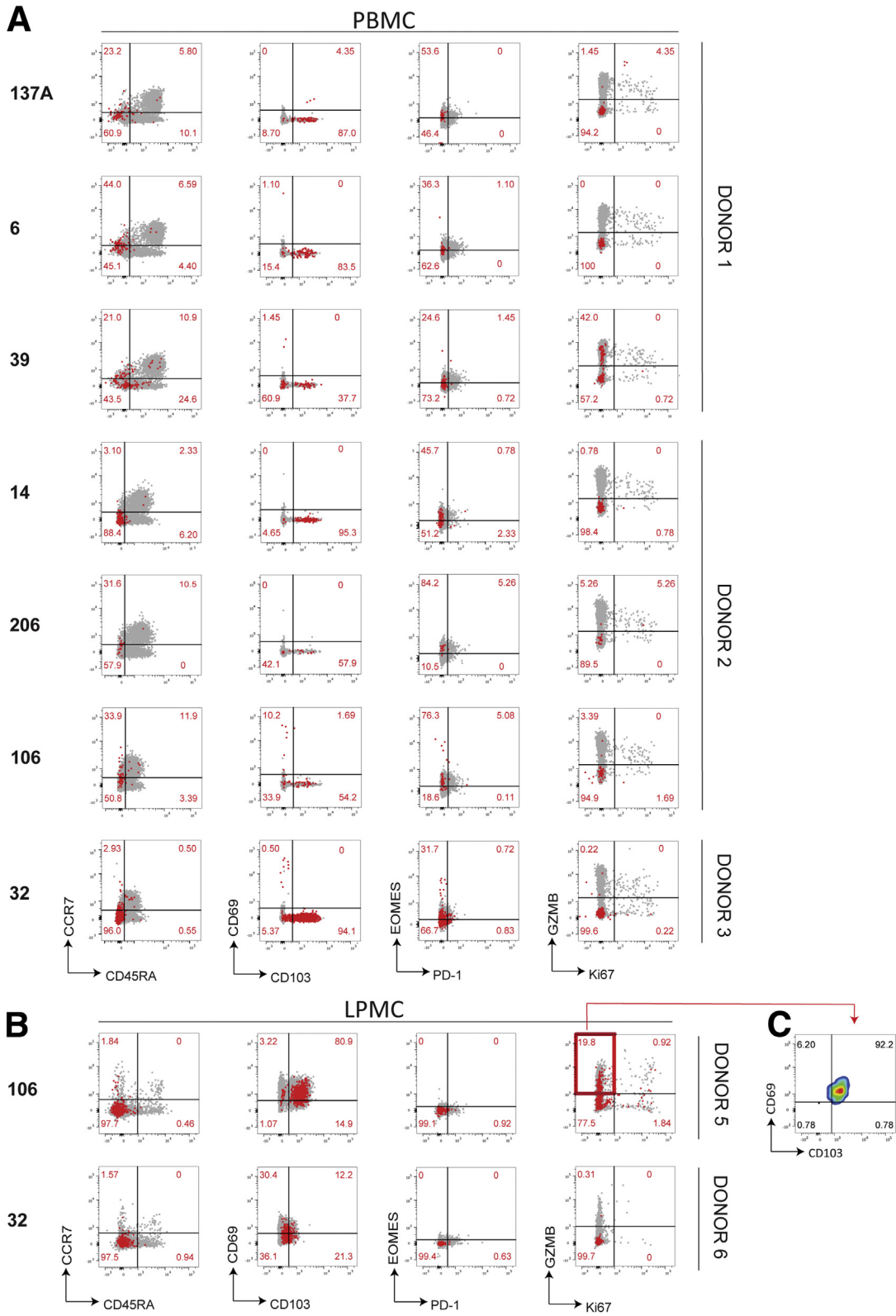
Figure 7. Phenotypic characterization of NoV-specific CD8$^+$ T cells. (*A*) PBMCs or (*B*) LPMCs were stained with tetramers and a panel of antibodies against memory, homing, exhaustion, proliferation, and cytotoxicity markers. Total live CD8$^+$ T cells are shown in *grey* with Tet$^+$ cells overlayed in *red*. Representative of 3 independent experiments.

was represented in our study. Moreover, this shared HLA type was present in Donor 3, who was a non-secretor and had an unclear exposure history, complicating comparisons (Figure 3C and D). Notably, epitope 32, which was restricted to HLA B*35:01, was not discovered by Hanajiri et al despite being conserved in the Sydney_2012 strain (Figure 4). Conversely, the B*35:01-restricted epitope described by Hanajiri et al (FPGEQLLFF) did not elicit a strong signal in our screen, even though it was present in our library (data not shown). One explanation for these discrepancies could be altered immunodominance hierarchy between individual subjects. This phenomenon has been described for influenza virus where presence of the B*27:05 antigen diminished binding of an otherwise immunodominant epitope to HLA A*02:01.[60] Another explanation for why we did not find the FPGEQLLFF epitope could be differences in exposure histories. Although we did not detect serologic responses from Donor 3, it is likely that his NoV immune repertoire was shaped by secretor-independent strains that were not represented in our VLP library. Such strains have been well-documented[27,61–65] and include members of GII.2 that harbor a glutamine deletion in the FPGE**Q**LLFF sequence (data not shown). This deletion is likely to impact binding to HLA B*35:01 by shortening the spacing between anchor residues, thus making it a non-dominant epitope for Donor 3. In contrast, the length and anchor positions of epitope 32 were largely conserved among GII.2 strains with only minor variation between aromatic residues (Phe versus Tyr) in position 9 (Table 3).

The importance of cellular immunity for NoV control has been clearly shown in the mouse model where depletion of CD4$^+$ or CD8$^+$ T cells enables viral persistence.[26] In humans, data from both immunocompromised and immunocompetent hosts suggest a similar need for broad cellular immunity to achieve viral control.[29,66–69] At the same time, antibodies remain critical for MNV control,[70] and a functional T-cell response is not always sufficient for viral clearance.[2] Similarly, immunocompetent humans can have prolonged viral shedding after acute infection, possibly suggesting that NoVs can circumvent humoral and cellular immunity.[34,36–38] Indeed, the high degree of HLA class I epitope conservation among GII.4 viruses (Table 2) suggests that these sequences are not under immune pressure, and T cells alone cannot provide sufficient protection against NoV. Thus, NoVs have likely evolved strategies of T-cell evasion that do not rely on epitope changes. In mice, one such strategy is persistence in tuft cells, which provide an immune-privileged niche for viral replication.[39,45] In humans, the cellular target for acute and chronic NoV infection remains unknown, as do other host-virus interactions that may enable T-cell evasion, pointing to a need for future studies. Consistent with data from mice[2] and humans,[33] our limited phenotypic and functional analysis shows that NoV-specific T$_{CM}$ and T$_{EM}$ are polyfunctional (Figure 2) and do not show features of T-cell exhaustion (Figure 7). Although our observations derive from a small set of samples, it should now be possible to use tetramers to track NoV-specific CD8$^+$ T cells in larger cohorts at defined time points after infection. Such studies

could validate our findings and provide more comprehensive functional, transcriptional, and epigenetic analyses of NoV-specific T cells.

The tissue distribution and trafficking patterns of memory T cells are important determinants of their effectiveness, and several vaccination strategies have focused on promoting T$_{RM}$ formation at relevant mucosal surfaces.[71–74] Thus, an important question is whether preexisting virus-specific T$_{RM}$ after exposure to multiple GI or GII strains early in life correlate with future NoV susceptibility and disease severity. Similarly, the ability to elicit a robust T$_{RM}$ response may be an important metric for future NoV vaccine candidates. We were able to detect Tet$^+$ T$_{RM}$ in the intestinal LP (Figure 7), suggesting that such cells could play an important protective role. Future studies using tetramers and intestinal samples should build on these observations and fully define the location and microenvironment of NoV-specific T cells. If carried out in the context of a vaccine trial, such studies could be highly valuable in elucidating T$_{RM}$ correlates of NoV immunity.

Methods

Human Donors

PBMCs used for peptide library screening were obtained from 3 healthy adult volunteers with no significant medical history in accordance with the Institutional Review Board approval at the University of Pennsylvania (Donors 1–3, Table 1). PBMCs from 13 additional donors were obtained from the Human Immunology Core at the University of Pennsylvania (https://pathbio.med.upenn.edu/hic/site/) with limited clinical metadata available (Donors 7–19, Table 1). Duodenal organs and lymphoid tissues were obtained from deceased donors in accordance with Institutional Review Board approval of the Human Pancreas Analysis Program[75] (https://hpap.pmacs.upenn.edu/) (Donors 4–6, Table 1).

Blockade Antibody Detection

Serum samples were thawed, heat-inactivated at 56°C for 30 minutes, and stored at 4°C during testing. To determine blockade antibody titer (mean inhibitory concentration of 50%), enzyme immunoassay plates were coated with 10 µg/mL porcine gastric mucin (PGM) type III diluted in phosphate-buffered saline (PBS) and blocked with 5% Blotto in PBS-0.05% Tween 20. VLPs (0.25 µg/mL) were pretreated with decreasing 2-fold concentrations of serum for 1 hour before being added to the PGM-coated plates for 1 hour. Ligand-bound VLPs were detected with rabbit anti-VLP hyperimmune serum followed by anti-rabbit immunoglobulin G–horseradish peroxidase, and color developed with TMB substrate. Incubations were done at 37°C. The percent control binding was defined as binding in the presence of antibody pretreatment compared with binding in the absence of antibody pretreatment multiplied by 100. Samples that did not block at least 50% of VLP binding at the lowest dilution tested (10%) were assigned a titer of 5%, 0.5× the lower limit of detection. Each sample was assayed in 10-fold serial dilution in a minimum of 2

Table 5. Antibodies Used

Antibody	Clone	Source	Catalog #
Anti-hu CD4 PE/CY5	OKT4	Biolegend	317411
Anti-hu CD8 BV785	RPA-T8	BD Biosciences	563823
Anti-hu CD3 BV570	UCHT1	Biolegend	300436
Anti-hu CD14 V500	M5E2	BD Biosciences	561391
Anti-hu CD16 V500	3G8	BD Biosciences	561393
Anti-hu CD19 V500	HIB19	BD Biosciences	561125
Ghost Dye Violet 510	N/A	Tonbo Bioscieces	13-0870-T500
Anti-hu CD103 AF488	Ber-ACT8	Biolegend	350208
Anti-hu Eomes PerCP e-fluor710	WD1928	eBioscience	46-4877-42
Anti-hu GranzymeB PE-TxRd	GB11	Invitrogen	GRB17
Anti-hu Ki-67 PECy7	20Raj1	eBioscience	25-5699-41
Anti-hu CD69 AF700	FN50	Biolegend	310922
Anti-hu CCR7 APC-Cy7	GO43H7	Biolegend	353211
Anti-hu IFNG	B27	Biolegend	506516
Anti-hu TNFA	Mab1	Biolegend	502930

independent experiments. Blockade data were fit using sigmoidal dose response analysis of normalized non-linear data, and serum mean inhibitory concentration of 50% with 95% confidence intervals was calculated in GraphPad Prism 8.0.2 (San Diego, CA).

Peripheral Blood Mononuclear Cell Isolation

Blood was drawn in a vacutainer containing sodium heparin and diluted 1:1 with $1\times$ PBS (Corning-Cellgro, Corning, NY). Up to 25 mL of diluted sample was loaded onto Sepmate50 tubes (Stemcell Technologies, Vancouver, Canada) containing 15 mL density gradient Lymphoprep (Stemcell Technologies). Samples were centrifuged at 1500 rpm for 10 minutes at room temperature. Cells were washed with RPMI 1640 (Corning-Cellgro) + 2% fetal bovine serum (FBS) (GeminiBio, Calabasas, CA) and resuspended in freezing medium (90% FBS + 10% dimethyl sulfoxide [DMSO]). Samples were gradually cooled in a Mr. Frosty container (Thermo Fisher Scientific, Waltham, MA) with 100% isopropyl alcohol and kept at –80°C for up to 2 weeks or at –150°C for longer-term storage.

Lamina Propria Mononuclear Cell Isolation

Intestinal samples were processed as previously described.[76] Duodenal tissue ($\sim$20 cm of length) was opened longitudinally and cleaned thoroughly from bile by using a cell lifter and paper towels. The tissue was rinsed in PBS, cut into small pieces ($\leq$1 cm^2), and distributed into eight 50-mL conical tubes. After washing once in Epithelial Strip Buffer ($1\times$ PBS, 5 mmol/L EDTA, 1 mmol/L dithiothreitol, 5% FBS) at 37°C, the tissue was incubated in 30 mL fresh Strip Buffer per tube in a 37°C shaker for 90 minutes. After epithelial stripping, the duodenal tissue was rinsed in 20 mL cold Wash Buffer (RPMI, 2% FBS, 1% L-Glut, 1% Pen/Strep) and incubated in Digest Buffer consisting of Wash Buffer with 1 mg/mL collagenase type 4 (Worthington

LS004188; Worthington Biochemical, Lakewood, NJ), 1 mg/mL trypsin inhibitor (Worthington LS003587), and 50 μg/mL DNase I (Worthington LS002139) for 120 minutes in a 37°C shaker. After digestion, the samples were passed through a 70-μm cell strainer and washed in 20 mL cold Wash Buffer. The samples were then resuspended in 30 mL of 40% Percoll (Sigma-Aldrich, St Louis, MO) prepared in Wash Buffer and centrifuged for 30 minutes at room temperature at 600g with acceleration and deceleration set to 0. After centrifugation, the mucus and Percoll layers were carefully removed, and the LPMCs were washed twice with cold Wash Buffer and counted. LPMCs were finally resuspended in freezing medium (90% FBS + 10% DMSO), gradually cooled in a Mr. Frosty container (Thermo Fisher Scientific) with 100% isopropyl alcohol, and stored at –80°C for up to 2 weeks or at –150°C long term.

Mesenteric Lymph Node and Splenocyte Isolation

MLN samples were placed in a culture dish containing RPMI 1640 with 10% FBS and 1:100 DNase I (Roche, Basel, Germany). SPL were placed in RPMI 1640 with 10% FBS, 1:100 DNase I, and 1 mg/mL collagenase D (Sigma-Aldrich). The samples were rinsed, and fatty tissue was removed by using fine forceps. The tissues were then cut into small pieces. MLN samples were placed in a 70-μm cell strainer over a 50-mL conical tube and smashed using a 5-mL syringe piston. The cell strainer was washed twice with 10 mL medium. Cells were then spun down and resuspended in freezing medium (90% FBS+ 10% DMSO). SPL samples were placed in gentle MACS tubes and dissociated with a gentle MACS Dissociator (Miltenyi Biotec, Bergisch Gladbach, Germany). This was followed by 15-minute incubation at 37°C and a repeat dissociation. The suspension was passed through 100-μm cell strainer into 50-mL conical tube. The cells were washed and resuspended in 10 mL ACK

lysis buffer (Fisher Scientific, Pittsburgh, PA) for 5 minutes. After quenching with Wash Buffer, the cells were passed through 70-μm cell strainer and washed. The pellet was resuspended in 10 mL medium (RPMI 1640 with 10% FBS) and overlayed carefully on 10 mL Ficoll in fresh 50-mL conical tube. The sample was centrifuged at 2200 rpm at room temperature for 20 minutes with acceleration and deceleration set to 0. The cells were finally resuspended in freezing medium and frozen as described above.

Peptide Libraries

Overlapping peptide libraries were designed on the basis of the GII.4 Farmington Hills strain (Genbank accession number AY502023). Peptides were 15 amino acids long and spanned each ORF, with neighboring peptides overlapping by 10 residues. All peptides were synthesized by GenScript (Piscataway, NJ), resuspended in DMSO at a concentration of 40 mg/mL, and stored at –80°C. Overlapping peptide pools containing up to 25 peptides were generated as shown in Figure 3. Pools were made in serum-free RPMI 1640 with each peptide at 0.8 μg/mL and stored at –80°C.

Peptide Stimulations

PBMCs were thawed and washed with RPMI containing 10% FBS and 1% Pen/Strep. Thawed cells were resuspended in 2× culture medium consisting of RPMI 1640 with 20% FBS, 2% Pen strep, 40 mmol/L HEPES, 2 mmol/L sodium pyruvate, 200 μmol/L non-essential amino acid, and 0.1 mmol/L β-mercaptoethanol. Cells were then stimulated by adding equal volume of 0.8 μg/mL peptide mix in serum-free RPMI for a final peptide concentration of 0.4 μg/mL. IL2 was added to a final concentration of 100 U/μL, and cells were incubated at 37°C and 5% CO_2. Cells were cultured for 10 days, with additional IL2 added on days 3, 5, and 7, and culture medium changed on day 5. On day 10, the cells were re-stimulated with peptide(s) at a final concentration of 0.4 μg/mL in the presence of GolgiPlug (BD Biosciences, San Jose, CA) for 18 hours.

Flow Cytometry

Surface antibody mixes were prepared in fluorescence-activated cell sorter (FACS) buffer (PBS with 0.05% FBS). Cells were washed in FACS buffer, incubated with surface antibodies for 30 minutes at room temperature, and washed again with FACS buffer. Next, cells were permeabilized using a Fix/Perm kit (BD Biosciences) for 30 minutes at room temperature, followed by 2 washes. Intracellular antibody mixes were prepared in Fix/Perm Wash buffer, and cells were stained for 1 hour, washed, and resuspended in FACS buffer. Data were acquired on an LSR II flow cytometer (BD Immunocytometry Systems, San Jose, CA). Data analyses were done by using FlowJo v10.7 (TreeStar, San Carlos, CA). Antibodies used are listed in Table 5.

Tetramers

Biotinylated monomers were synthesized at the NIH Tetramer Core Facility (Atlanta, GA). Monomers at a concentration of 200 μg/100 μL were tetramerized by adding aliquots of streptavidin-APC or streptavidin-PE at 1 mg/mL (Fisher Scientific). Aliquots of 17.6 μL streptavidin-APC or 31.9 μL streptavidin-PE were added and mixed gently, followed by incubation in the dark at room temperature for 10 minutes. This process was repeated 10 times. Tetramer staining was done at 1:200 dilution.

References

1. Debbink K, Lindesmith LC, Donaldson EF, Baric RS. Norovirus immunity and the great escape. PLoS Pathog 2012;8:e1002921.
2. Tomov VT, Palko O, Lau CW, Pattekar A, Sun Y, Tacheva R, Bengsch B, Manne S, Cosma GL, Eisenlohr LC, Nice TJ, Virgin HW, Wherry EJ. Differentiation and protective capacity of virus-specific CD8(+) T cells suggest murine norovirus persistence in an immune-privileged enteric niche. Immunity 2017; 47:723–738 e5.
3. Patel MM, Widdowson MA, Glass RI, Akazawa K, Vinje J, Parashar UD. Systematic literature review of role of noroviruses in sporadic gastroenteritis. Emerg Infect Dis 2008;14:1224–1231.
4. Payne DC, Vinje J, Szilagyi PG, Edwards KM, Staat MA, Weinberg GA, Hall CB, Chappell J, Bernstein DI, Curns AT, Wikswo M, Shirley SH, Hall AJ, Lopman B, Parashar UD. Norovirus and medically attended gastroenteritis in U.S. children. N Engl J Med 2013; 368:1121–1130.
5. Esposito S, Principi N. Norovirus vaccine: priorities for future research and development. Front Immunol 2020; 11:1383.
6. Mattison CP, Cardemil CV, Hall AJ. Progress on norovirus vaccine research: public health considerations and future directions. Expert Rev Vaccines 2018; 17:773–784.
7. Sosnovtsev SV, Belliot G, Chang KO, Prikhodko VG, Thackray LB, Wobus CE, Karst SM, Virgin HW, Green KY. Cleavage map and proteolytic processing of the murine norovirus nonstructural polyprotein in infected cells. J Virol 2006;80:7816–7831.
8. Prasad BV, Hardy ME, Dokland T, Bella J, Rossmann MG, Estes MK. X-ray crystallographic structure of the Norwalk virus capsid. Science 1999; 286:287–290.
9. Conley MJ, McElwee M, Azmi L, Gabrielsen M, Byron O, Goodfellow IG, Bhella D. Calicivirus VP2 forms a portal-like assembly following receptor engagement. Nature 2019;565:377–381.
10. Chhabra P, de Graaf M, Parra GI, Chan MC, Green K, Martella V, Wang Q, White PA, Katayama K, Vennema H, Koopmans MPG, Vinje J. Updated classification of norovirus genogroups and genotypes. J Gen Virol 2019; 100:1393–1406.
11. Son H, Jeong HS, Cho M, Lee J, Lee H, Yoon K, Jeong AY, Jung S, Kim K, Cheon DS. Seroepidemiology of predominant norovirus strains circulating in Korea by using recombinant virus-like particle antigens. Foodborne Pathog Dis 2013;10:461–466.

12. Karst SM, Baric RS. What is the reservoir of emergent human norovirus strains? J Virol 2015;89:5756–5759.

13. Nordgren J, Svensson L. Genetic susceptibility to human norovirus infection: an update. Viruses 2019;11(3).

14. Lindesmith LC, McDaniel JR, Changela A, Verardi R, Kerr SA, Costantini V, Brewer-Jensen PD, Mallory ML, Voss WN, Boutz DR, Blazeck JJ, Ippolito GC, Vinje J, Kwong PD, Georgiou G, Baric RS. Sera antibody repertoire analyses reveal mechanisms of broad and pandemic strain neutralizing responses after human norovirus vaccination. Immunity 2019;50:1530–1541 e8.

15. Parker TD, Kitamoto N, Tanaka T, Hutson AM, Estes MK. Identification of genogroup I and genogroup II broadly reactive epitopes on the norovirus capsid. J Virol 2005; 79:7402–7409.

16. Karst SM, Wobus CE, Goodfellow IG, Green KY, Virgin HW. Advances in norovirus biology. Cell Host Microbe 2014;15:668–680.

17. Rouquier S, Lowe JB, Kelly RJ, Fertitta AL, Lennon GG, Giorgi D. Molecular cloning of a human genomic region containing the H blood group alpha(1,2)fucosyltransferase gene and two H locus-related DNA restriction fragments: isolation of a candidate for the human secretor blood group locus. J Biol Chem 1995;270:4632–4639.

18. Lindesmith L, Moe C, Marionneau S, Ruvoen N, Jiang X, Lindblad L, Stewart P, LePendu J, Baric R. Human susceptibility and resistance to Norwalk virus infection. Nat Med 2003;9:548–553.

19. Johnson PC, Mathewson JJ, DuPont HL, Greenberg HB. Multiple-challenge study of host susceptibility to Norwalk gastroenteritis in US adults. J Infect Dis 1990; 161:18–21.

20. Parrino TA, Schreiber DS, Trier JS, Kapikian AZ, Blacklow NR. Clinical immunity in acute gastroenteritis caused by Norwalk agent. N Engl J Med 1977; 297:86–89.

21. Reeck A, Kavanagh O, Estes MK, Opekun AR, Gilger MA, Graham DY, Atmar RL. Serological correlate of protection against norovirus-induced gastroenteritis. J Infect Dis 2010;202:1212–1218.

22. Lindesmith LC, Ferris MT, Mullan CW, Ferreira J, Debbink K, Swanstrom J, Richardson C, Goodwin RR, Baehner F, Mendelman PM, Bargatze RF, Baric RS. Broad blockade antibody responses in human volunteers after immunization with a multivalent norovirus VLP candidate vaccine: immunological analyses from a phase I clinical trial. PLoS Med 2015;12:e1001807.

23. Simmons K, Gambhir M, Leon J, Lopman B. Duration of immunity to norovirus gastroenteritis. Emerg Infect Dis 2013;19:1260–1267.

24. Atmar RL, Bernstein DI, Harro CD, Al-Ibrahim MS, Chen WH, Ferreira J, Estes MK, Graham DY, Opekun AR, Richardson C, Mendelman PM. Norovirus vaccine against experimental human Norwalk virus illness. N Engl J Med 2011;365:2178–2187.

25. Ramirez K, Wahid R, Richardson C, Bargatze RF, El-Kamary SS, Sztein MB, Pasetti MF. Intranasal vaccination with an adjuvanted Norwalk virus-like particle vaccine elicits antigen-specific B memory responses in human adult volunteers. Clin Immunol 2012;144:98–108.

26. Chachu KA, LoBue AD, Strong DW, Baric RS, Virgin HW. Immune mechanisms responsible for vaccination against and clearance of mucosal and lymphatic norovirus infection. PLoS Pathog 2008;4:e1000236.

27. Lindesmith L, Moe C, Lependu J, Frelinger JA, Treanor J, Baric RS. Cellular and humoral immunity following Snow Mountain virus challenge. J Virol 2005;79:2900–2909.

28. Lindesmith LC, Donaldson E, Leon J, Moe CL, Frelinger JA, Johnston RE, Weber DJ, Baric RS. Heterotypic humoral and cellular immune responses following Norwalk virus infection. J Virol 2010; 84:1800–1815.

29. Lindesmith LC, Brewer-Jensen PD, Mallory ML, Jensen K, Yount BL, Costantini V, Collins MH, Edwards CE, Sheahan TP, Vinje J, Baric RS. Virus-host interactions between nonsecretors and human norovirus. Cell Mol Gastroenterol Hepatol 2020;10:245–267.

30. LoBue AD, Lindesmith LC, Baric RS. Identification of cross-reactive norovirus CD4+ T cell epitopes. J Virol 2010;84:8530–8538.

31. Malm M, Tamminen K, Vesikari T, Blazevic V. Norovirus-specific memory T cell responses in adult human donors. Front Microbiol 2016;7:1570.

32. Malm M, Vesikari T, Blazevic V. Identification of a first human norovirus CD8(+) T cell epitope restricted to HLA-A(*)0201 allele. Front Immunol 2018;9:2782.

33. Hanajiri R, Sani GM, Saunders D, Hanley PJ, Chopra A, Mallal SA, Sosnovtsev SV, Cohen JI, Green KY, Bollard CM, Keller MD. Generation of norovirus-specific T cells from human donors with extensive cross-reactivity to variant sequences: implications for immunotherapy. J Infect Dis 2020;221:578–588.

34. Rockx B, De Wit M, Vennema H, Vinje J, De Bruin E, Van Duynhoven Y, Koopmans M. Natural history of human calicivirus infection: a prospective cohort study. Clin Infect Dis 2002;35:246–253.

35. Patterson T, Hutchings P, Palmer S. Outbreak of SRSV gastroenteritis at an international conference traced to food handled by a post-symptomatic caterer. Epidemiol Infect 1993;111:157–162.

36. Atmar RL, Opekun AR, Gilger MA, Estes MK, Crawford SE, Neill FH, Graham DY. Norwalk virus shedding after experimental human infection. Emerg Infect Dis 2008;14:1553–1557.

37. Murata T, Katsushima N, Mizuta K, Muraki Y, Hongo S, Matsuzaki Y. Prolonged norovirus shedding in infants < or =6 months of age with gastroenteritis. Pediatr Infect Dis J 2007;26:46–49.

38. Pang XL, Joensuu J, Vesikari T. Human calicivirus-associated sporadic gastroenteritis in Finnish children less than two years of age followed prospectively during a rotavirus vaccine trial. Pediatr Infect Dis J 1999;18:420–426.

39. Wilen CB, Lee S, Hsieh LL, Orchard RC, Desai C, Hykes BL Jr, McAllaster MR, Balce DR, Feehley T, Brestoff JR, Hickey CA, Yokoyama CC, Wang YT, MacDuff DA, Kreamalmayer D, Howitt MR, Neil JA, Cadwell K, Allen PM, Handley SA, van Lookeren Campagne M, Baldridge MT, Virgin HW. Tropism for tuft cells determines immune promotion of norovirus pathogenesis. Science 2018;360:204–208.

40. Graziano VR, Walker FC, Kennedy EA, Wei J, Ettayebi K, Strine MS, Filler RB, Hassan E, Hsieh LL, Kim AS, Kolawole AO, Wobus CE, Lindesmith LC, Baric RS, Estes MK, Orchard RC, Baldridge MT, Wilen CB. CD300lf is the primary physiologic receptor of murine norovirus but not human norovirus. PLoS Pathog 2020;16:e1008242.

41. Widdowson MA, Cramer EH, Hadley L, Bresee JS, Beard RS, Bulens SN, Charles M, Chege W, Isakbaeva E, Wright JG, Mintz E, Forney D, Massey J, Glass RI, Monroe SS. Outbreaks of acute gastroenteritis on cruise ships and on land: identification of a predominant circulating strain of norovirus—United States, 2002. J Infect Dis 2004;190:27–36.

42. Ruan GP, Ma L, Wen Q, Luo W, Zhou MQ, Wang XN. A modified peptide stimulation method for efficient amplification of cytomegalovirus (CMV)-specific CTLs. Cell Mol Immunol 2008;5:197–201.

43. Sanchez-Trincado JL, Gomez-Perosanz M, Reche PA. Fundamentals and methods for T- and B-cell epitope prediction. J Immunol Res 2017;2017:2680160.

44. Nordgren J, Kindberg E, Lindgren PE, Matussek A, Svensson L. Norovirus gastroenteritis outbreak with a secretor-independent susceptibility pattern, Sweden. Emerg Infect Dis 2010;16:81–87.

45. Tomov VT, Osborne LC, Dolfi DV, Sonnenberg GF, Monticelli LA, Mansfield K, Virgin HW, Artis D, Wherry EJ. Persistent enteric murine norovirus infection is associated with functionally suboptimal virus-specific CD8 T cell responses. J Virol 2013;87:7015–7031.

46. Vita R, Zarebski L, Greenbaum JA, Emami H, Hoof I, Salimi N, Damle R, Sette A, Peters B. The immune epitope database 2.0. Nucleic Acids Res 2010;38-(database issue):D854–D862.

47. Reynisson B, Alvarez B, Paul S, Peters B, Nielsen M. NetMHCpan-4.1 and NetMHCIIpan-4.0: improved predictions of MHC antigen presentation by concurrent motif deconvolution and integration of MS MHC eluted ligand data. Nucleic Acids Res 2020;48(W1):W449–W454.

48. Burrows SR, Rossjohn J, McCluskey J. Have we cut ourselves too short in mapping CTL epitopes? Trends Immunol 2006;27:11–16.

49. Szabo PA, Miron M, Farber DL. Location, location, location: tissue resident memory T cells in mice and humans. Sci Immunol 2019;4(34).

50. Luoma AM, Suo S, Williams HL, Sharova T, Sullivan K, Manos M, Bowling P, Hodi FS, Rahma O, Sullivan RJ, Boland GM, Nowak JA, Dougan SK, Dougan M, Yuan GC, Wucherpfennig KW. Molecular pathways of colon inflammation induced by cancer immunotherapy. Cell 2020;182:655–671 e22.

51. Park SL, Zaid A, Hor JL, Christo SN, Prier JE, Davies B, Alexandre YO, Gregory JL, Russell TA, Gebhardt T, Carbone FR, Tscharke DC, Heath WR, Mueller SN, Mackay LK. Local proliferation maintains a stable pool of tissue-resident memory T cells after antiviral recall responses. Nat Immunol 2018; 19:183–191.

52. Rosato PC, Wijeyesinghe S, Stolley JM, Masopust D. Integrating resident memory into T cell differentiation models. Curr Opin Immunol 2020;63:35–42.

53. Martin MD, Badovinac VP. Defining memory CD8 T cell. Front Immunol 2018;9:2692.

54. Kirk MD, Pires SM, Black RE, Caipo M, Crump JA, Devleesschauwer B, Dopfer D, Fazil A, Fischer-Walker CL, Hald T, Hall AJ, Keddy KH, Lake RJ, Lanata CF, Torgerson PR, Havelaar AH, Angulo FJ. World Health Organization estimates of the global and regional disease burden of 22 foodborne bacterial, protozoal, and viral diseases, 2010: a data synthesis. PLoS Med 2015;12:e1001921.

55. Giersing BK, Modjarrad K, Kaslow DC, Moorthy VS; Committee WHOPDfVA, Committee WHOPDfVPDA. Report from the World Health Organization's Product Development for Vaccines Advisory Committee (PDVAC) meeting, Geneva, 7-9th Sep 2015. Vaccine 2016; 34:2865–2869.

56. Ettayebi K, Crawford SE, Murakami K, Broughman JR, Karandikar U, Tenge VR, Neill FH, Blutt SE, Zeng XL, Qu L, Kou B, Opekun AR, Burrin D, Graham DY, Ramani S, Atmar RL, Estes MK. Replication of human noroviruses in stem cell-derived human enteroids. Science 2016;353:1387–1393.

57. Jones MK, Grau KR, Costantini V, Kolawole AO, de Graaf M, Freiden P, Graves CL, Koopmans M, Wallet SM, Tibbetts SA, Schultz-Cherry S, Wobus CE, Vinje J, Karst SM. Human norovirus culture in B cells. Nat Protoc 2015;10:1939–1947.

58. Gerdemann U, Katari UL, Papadopoulou A, Keirnan JM, Craddock JA, Liu H, Martinez CA, Kennedy-Nasser A, Leung KS, Gottschalk SM, Krance RA, Brenner MK, Rooney CM, Heslop HE, Leen AM. Safety and clinical efficacy of rapidly-generated trivirus-directed T cells as treatment for adenovirus, EBV, and CMV infections after allogeneic hematopoietic stem cell transplant. Mol Ther 2013;21:2113–2121.

59. Leen AM, Myers GD, Sili U, Huls MH, Weiss H, Leung KS, Carrum G, Krance RA, Chang CC, Molldrem JJ, Gee AP, Brenner MK, Heslop HE, Rooney CM, Bollard CM. Monoculture-derived T lymphocytes specific for multiple viruses expand and produce clinically relevant effects in immunocompromised individuals. Nat Med 2006;12:1160–1166.

60. Sant S, Quinones-Parra SM, Koutsakos M, Grant EJ, Loudovaris T, Mannering SI, Crowe J, van de Sandt CE, Rimmelzwaan GF, Rossjohn J, Gras S, Loh L, Nguyen THO, Kedzierska K. HLA-B*27:05 alters immunodominance hierarchy of universal influenza-specific CD8+ T cells. PLoS Pathog 2020;16:e1008714.

61. Ayouni S, Estienney M, Sdiri-Loulizi K, Ambert-Balay K, de Rougemont A, Aho S, Hammami S, Aouni M, Guediche MN, Pothier P, Belliot G. Relationship between GII.3 norovirus infections and blood group antigens in young children in Tunisia. Clin Microbiol Infect 2015; 21:874 e1–874 e8.

62. Jin M, He Y, Li H, Huang P, Zhong W, Yang H, Zhang H, Tan M, Duan ZJ. Two gastroenteritis outbreaks caused by GII noroviruses: host susceptibility and HBGA phenotypes. PLoS One 2013;8:e58605.

63. Karangwa CK, Parra GI, Bok K, Johnson JA, Levenson EA, Green KY. Sequential gastroenteritis

outbreaks in a single year caused by norovirus genotypes GII.2 and GII.6 in an institutional setting. Open Forum Infect Dis 2017;4:ofx236.

64. Van Trang N, Vu HT, Le NT, Huang P, Jiang X, Anh DD. Association between norovirus and rotavirus infection and histo-blood group antigen types in Vietnamese children. J Clin Microbiol 2014;52:1366–1374.

65. Zhang XF, Huang Q, Long Y, Jiang X, Zhang T, Tan M, Zhang QL, Huang ZY, Li YH, Ding YQ, Hu GF, Tang S, Dai YC. An outbreak caused by GII.17 norovirus with a wide spectrum of HBGA-associated susceptibility. Sci Rep 2015;5:17687.

66. Brown LK, Clark I, Brown JR, Breuer J, Lowe DM. Norovirus infection in primary immune deficiency. Rev Med Virol 2017;27:e1926.

67. Brown LK, Ruis C, Clark I, Roy S, Brown JR, Albuquerque AS, Patel SY, Miller J, Karim MY, Dervisevic S, Moore J, Williams CA, Cudini J, Moreira F, Neild P, Seneviratne SL, Workman S, Toumpanakis C, Atkinson C, Burns SO, Breuer J, Lowe DM. A comprehensive characterization of chronic norovirus infection in immunodeficient hosts. J Allergy Clin Immunol 2019;144:1450–1453.

68. Newman KL, Moe CL, Kirby AE, Flanders WD, Parkos CA, Leon JS. Norovirus in symptomatic and asymptomatic individuals: cytokines and viral shedding. Clin Exp Immunol 2016;184:347–357.

69. Siebenga JJ, Beersma MF, Vennema H, van Biezen P, Hartwig NJ, Koopmans M. High prevalence of prolonged norovirus shedding and illness among hospitalized patients: a model for in vivo molecular evolution. J Infect Dis 2008;198:994–1001.

70. Chachu KA, Strong DW, LoBue AD, Wobus CE, Baric RS, HWt Virgin. Antibody is critical for the clearance of murine norovirus infection. J Virol 2008; 82:6610–6617.

71. Cuburu N, Graham BS, Buck CB, Kines RC, Pang YY, Day PM, Lowy DR, Schiller JT. Intravaginal immunization with HPV vectors induces tissue-resident CD8+ T cell responses. J Clin Invest 2012;122:4606–4620.

72. Shin H, Iwasaki A. A vaccine strategy that protects against genital herpes by establishing local memory T cells. Nature 2012;491:463–467.

73. Tan HX, Wheatley AK, Esterbauer R, Jegaskanda S, Glass JJ, Masopust D, De Rose R, Kent SJ. Induction of vaginal-resident HIV-specific CD8 T cells with mucosal prime-boost immunization. Mucosal Immunol 2018; 11:994–1007.

74. Zens KD, Chen JK, Farber DL. Vaccine-generated lung tissue-resident memory T cells provide heterosubtypic protection to influenza infection. JCI Insight 2016;1: e85832.

75. Kaestner KH, Powers AC, Naji A, Consortium H, Atkinson MA. NIH initiative to improve understanding of the pancreas, islet, and autoimmunity in type 1 diabetes: The Human Pancreas Analysis Program (HPAP). Diabetes 2019;68:1394–1402.

76. Konnikova L, Boschetti G, Rahman A, Mitsialis V, Lord J, Richmond C, Tomov VT, Gordon W, Jelinsky S, Canavan J, Liss A, Wall S, Field M, Zhou F, Goldsmith JD, Bewtra M, Breault DT, Merad M, Snapper SB. High-dimensional immune phenotyping and transcriptional analyses reveal robust recovery of viable human immune and epithelial cells from frozen gastrointestinal tissue. Mucosal Immunol 2018;11:1684–1693.

Correspondence
Address correspondence to: Vesselin Tomov, MD, PhD, Department of Medicine, Division of Gastroenterology, University of Pennsylvania, Perelman School of Medicine, 421 Curie Boulevard, BRB 313, Philadelphia, Pennsylvania 19103. e-mail: tomovv@pennmedicine.upenn.edu; fax: (215) 349-5915.